Bio-Design and Manufacturing (2022) 5:757–785
https://doi.org/10.1007/s42242-022-00201-7

REVIEW

Structural design and mechanical performance of composite vascular grafts

Abdul Wasy Zia[1] · Rong Liu[1] · Xinbo Wu[1]

Received: 7 November 2021 / Accepted: 8 May 2022 / Published online: 23 August 2022

Abstract

This study reviews the state of the art in structural design and the corresponding mechanical behaviours of composite vascular grafts. We critically analyse surface and matrix designs composed of layered, embedded, and hybrid structures along the radial and longitudinal directions; materials and manufacturing techniques, such as tissue engineering and the use of textiles or their combinations; and the corresponding mechanical behaviours of composite vascular grafts in terms of their physical–mechanical properties, especially their stress–strain relationships and elastic recovery. The role of computational studies is discussed with respect to optimizing the geometrics designs and the corresponding mechanical behaviours to satisfy specialized applications, such as those for the aorta and its subparts. Natural and synthetic endothelial materials yield improvements in the mechanical and biological compliance of composite graft surfaces with host arteries. Moreover, the diameter, wall thickness, stiffness, compliance, tensile strength, elasticity, and burst strength of the graft matrix are determined depending on the application and the patient. For composite vascular grafts, hybrid architectures are recommended featuring multiple layers, dimensions, and materials to achieve the desired optimal flexibility and function for complying with user-specific requirements. Rapidly emerging artificial intelligence and big data techniques for diagnostics and the three-dimensional (3D) manufacturing of vascular grafts will likely yield highly compliant, subject-specific, long-lasting, and economical vascular grafts in the near-future.

Graphic abstract

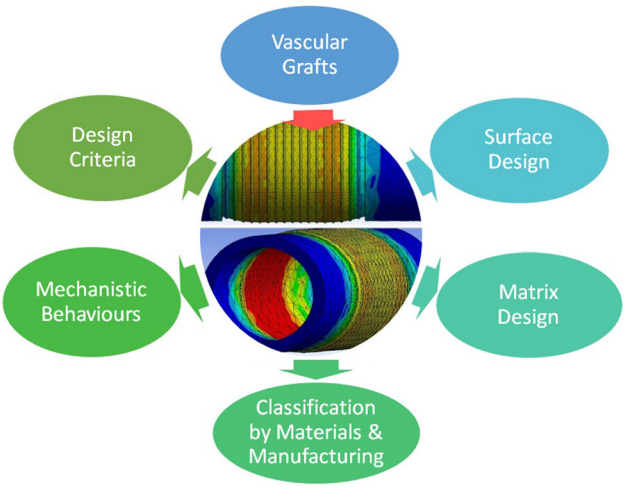

Keywords Vascular grafts · Surface design · Structural design · Composite materials · Mechanical properties

✉ Rong Liu
rong.liu@polyu.edu.hk

[1] School of Fashion and Textiles, The Hong Kong Polytechnic University, Hung Hom, Kowloon, Hong Kong SAR, China

Introduction

Artificial implants

Human body parts are subject to wear and tear and degenerate due to aging and disease. When natural body parts become dysfunctional, they can be replaced with long-lasting artificial implants. For example, cochlear implants are used to provide the sensation of sound for people with severe hearing loss by bypassing the ear and directly stimulating the cochlear nerve [1]. Intacs® corneal implants are used to reverse vision loss [2, 3] caused by age-induced changes in retinal shape. Endosteal [4], subperiosteal [5], and zygomatic [6] dental implants are used to treat teeth affected by plaque, decay, cavities, gingivitis, and periodontitis due to diabetes, hormonal changes [7, 8], acid reflux [9], infections [10], smoking, poor hygiene, or the adverse effects of medications [11]. Furthermore, lumbar disc implants [12] are used to treat degenerative lumbar disc diseases; prosthetic arthroplasty is performed to replace hip [13] and knee [14] joints, and acetabular implants [15] are used to repair hip or acetabular fractures. As is the case with other organs, the cardiovascular system is vulnerable to specific conditions, such as peripheral artery disease [16] or cerebrovascular disease [17], which reduce blood circulation in various areas of the body and can be treated with stents, heart valves, and vascular grafts [18]. Ceramic- and metal-based coatings are commonly applied to implants for various purposes, such as improving biocompatibility [19], imparting antimicrobial properties [20], reducing friction [21], and creating resistance to corrosion [22]. Figure 1 presents an overview of the various artificial implants (cochlear implants, corneal implants, dental implants, prosthetic shoulders, cardiovascular implants, pacemakers, lumbar disc implants, acetabular implants, prosthetic arthroplasty, hip and knee joints, and bone plates) and the treatment of corresponding diseases.

Vascular disorders and usability of composite vascular grafts

Statistics suggest that approximately two million people worldwide have end-stage renal disease. Further, chronic kidney diseases (CKD), diabetes, and other similar chronic diseases contribute to the increasing incidence of vascular disorders. For example, the CKD rate alone stood at approximately 12% in 2007, and it was projected to increase to 24% by 2035 [23]. The rapid growth rates of these diseases are fostering a demand for vascular grafts. Correspondingly, the global vascular graft market is expected to expand at a compounded annual growth rate of 6.2% between 2022 and 2027 [24]. Similarly, another market research report also suggests that the global revenue for the vascular graft market stood at $4.1 billion in 2016, and it is expected to grow to $6.2 billion by 2023 [25]. It has been estimated that North America will account for the highest share of the global vascular market owing to its higher prevalence rates of diabetes, CKDs, and cardiovascular diseases [26]. Researchers are therefore reporting new technological and material advancements in the context of vascular grafts, such as the potentials to use polyester and expanded polytetrafluoroethylene [27] for manufacturing vascular grafts to meet market demands.

Cardiovascular implants, such as stents, heart valves, and vascular grafts, are essential for treating cardiovascular diseases, including peripheral artery disease, cerebrovascular disease, and coronary heart diseases. These conditions generally result from blockages in the arteries, which limit the circulation of blood to various areas of the body. Stents are used to widen arteries and to open blockages without replacing the natural arteries, whereas vascular grafts are prosthetic implants that either bypass or replace natural blood vessels. Blood vessels usually dilate with age and may rupture under high blood pressure. Associated clinical factors include swelling and intimal hyperplasia [28]. The thickness of the inner layer of a blood vessel and the likelihood of thrombi (clotting) gradually increase with time, and this process is influenced to a greater extent by lifestyle than by age or sex. Clots are formed when blood components combine with cholesterol and other contaminations and cause irregularities in blood flow. Vascular grafts vary in size depending on the body-part and person [29]. For example, smaller grafts have inner diameters of less than 5 mm [30] but more than 1 mm [31]. Larger vascular grafts have diameters greater than 5 mm, and in the case of aortic applications, graft diameters can be as large as 18–34 mm [32].

Figure 2 illustrates the behaviours of blood vessels under systolic and diastolic blood flow with and without a thrombus (the blockage is marked in yellow). A blood vessel expands during a systolic cycle and retracts during a diastolic cycle of blood flow (Figs. 2a and 2b). However, when the blood flow becomes turbulent due to thrombus formation [33] inside the vessel, blood flow through a normal blood vessel (Fig. 2c) is disrupted (Fig. 2d) because the turbulence exerts excessive hemodynamic shear stress and increases the surface tension [34] on the vessel walls. Meanwhile, the cross-sectional area of the blood vessel is reduced because of thrombus formation (Fig. 2d). The narrowed vascular cross section further reduces the blood-flow rate and adds excessive shear stress [35], which causes a gradual degradation of the blood vessels. The fragile layer of endothelial material that is in direct contact with the blood is most vulnerable to an increase in shear stress. The blood vessel continually expands and retracts [36] in each systolic and diastolic blood cycle, and therefore, the thrombus reduces the fatigue life of the blood vessel.

The theory of contact mechanics [37, 38] can explain the empirical findings that show that excessive shear stress [39, 40] reduces the fatigue life of blood vessels. The shear forces

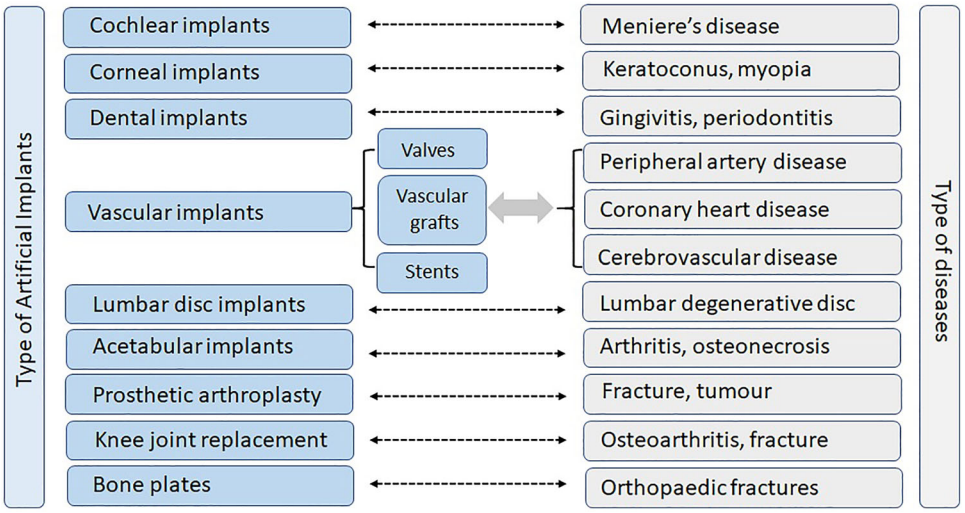

Fig. 1 Artificial implants commonly used in the human body and diseases requiring vascular grafts

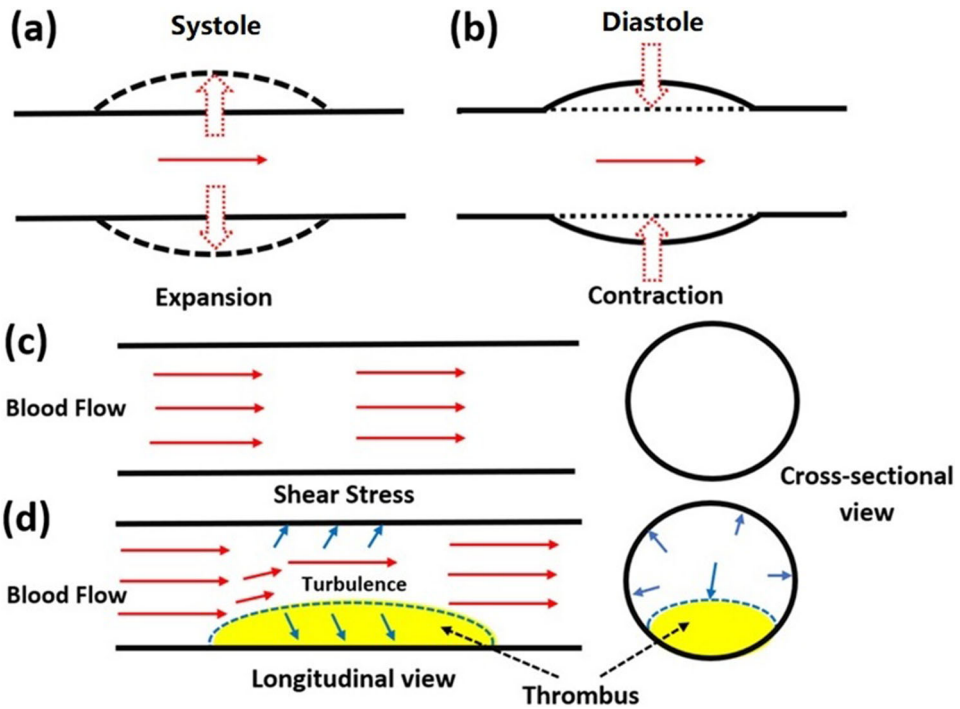

Fig. 2 Behaviours of blood vessels under **a** systolic and **b** diastolic blood flow, and **c** without and **d** with a thrombus

exerted by blood on vessel walls increase as the thrombus size increases, that is, the cross-sectional area of the blood flow decreases. Therefore, blood vessels tend to expand radially to maintain the blood flow rate. However, blood vessels have certain limitations in terms of radial and axial compliance, that is, in their ability to expand radially and axially. Therefore, blood circulation ceases once the thrombus completely clogs the vessel, and consequently the shear stresses exerted by blood may cause the vessel to burst or to bifurcate the thrombus, depending on the specific circumstances. A blocked blood vessel must be replaced or bypassed with a vascular graft to maintain blood supply to all parts of the body. The characteristics of such vascular grafts should be the same as or similar to those of the host artery, including their radial and axial compliance, burst strength, tensile strength, buckling, fatigue life, and elastic recovery.

The morphology, structure, and thickness of blood vessels vary by age, gender, and health-related factors. Therefore, a comparison of the mechanistic behaviours of small and large human arteries and of the commercially available and emerging composite vascular grafts should be carried out

for reference. A recent study [41] determined that small-diameter blood vessels have a higher ultimate strength than do large-diameter vessels. The ultimate tensile stress and corresponding straining percentage in the radial direction before failure were 4.1 MPa and 134%, respectively, for the internal mammary artery, 1.8 MPa and 242% for the saphenous vein, respectively, and 1–2 MPa and about 63%–76%, respectively, for the human femoral artery. An inverse trend has been observed in the longitudinal direction, with the internal mammary artery enduring 4.3 MPa of stress and 59% strain, and the saphenous vein exhibiting the highest strength under an ultimate stress of 6.3 MPa with an 83% strain. Small-diameter blood vessels (<5 mm) such as saphenous veins usually exhibit 0.4 strain and 0.2 MPa of stress at the pressure of 17.3–19.9 kPa [42]. Danpinid et al. suggested that the aorta (10–30 mm) has a transition strain of 0.03 for the corresponding Young's moduli of 0.07, 0.2 and 0.15 MPa in elastic lamellae, elastin-collagen, and collagen sub-layers, respectively [43], which is approximately 10 times lower than that of saphenous veins. Because the natural aorta has a layered structure, the Young's modulus changes depending on material properties. According to Zhao et al. [44], commercially available small-diameter stents (e.g. Johnson & Johnson's Palmaz–Schatz stent, Boston Scientific's Express Stent, Medtronic's S670 stent, and Guidant's Multilink Vision stent) with a 0.1 mm thickness, 3 mm outer diameter, and 16 mm length usually have a stent-induced maximum Von Mises stress of 0.09–0.17 MPa, a maximum principal stress of 0.08–0.22 MPa, and a maximum principal logarithm strain of 0.40–0.47. Similarly, commercially available, large-diameter stents (e.g. the GPS Carotid stent) with a 0.22 mm thickness, 10 mm outer diameter and 20 mm length have exhibited a 0.054 MPa maximum Von Mises stress, a 0.052 MPa maximum principal stress, and a 0.30 maximum principal logarithm strain.

Essential factors for composite vascular-graft design

A review of the literature published in the past several decades shows that material selection has generally been considered as a most common design criterion. The history of grafts can be tracked back to 1759, the year in which the first known lateral arteriography was performed [45]. A cardiovascular renaissance that took place from approximately 1940 and the use of polymer vascular grafts in the 1950s was the key milestones. Figure 3 highlights the differences in structure and radial compliance between natural blood vessels and synthetic vascular grafts. A mismatch between vessel and graft properties may cause life-threatening complications such as strokes [46], renal failure [47], endoleaks [48], swelling [49], leakage [50], and infections [51, 52]. Therefore, the manufacture of vascular-graft composites with mechanical properties similar to those of natural blood vessels remains essential.

Presently, vascular grafts are made using natural, synthetic, and biosynthetic materials individually, as well as in various combinations, to ensure that their mechanical properties are as similar as possible to those of natural arteries. Synthetic materials, including poly (ethylene terephthalate) (PET), polytetrafluoroethylene (PTFE), polyurethanes (PU), poly(ε-caprolactone) (PCL), polyamide (nylon), and their blends, are used to manufacture vascular grafts (e.g. the Dacron graft). These materials offer a range of mechanical and biomedical properties, which can be further tailored by using different manufacturing methods—such as extrusion—and by including or excluding scaffolding in the graft design. Artificial vascular grafts of various materials and dimensions are commercially available. However, some challenges must be addressed. For example, the material properties of natural arteries and those of artificial artery grafts made of Dacron or ePTFE may be mismatched. Standard commercial grafts lack the subject-specific customization required to respond to intraindividual and interindividual differences due to variations in physiological status caused by age, health, or disease severity such as problems persist among large-diameter abdominal aortic aneurysm repairs (e.g. those 30–45 mm in diameter). For example, knitted Dacron prostheses have high porosity and tissue ingrowth but dilate over time, which entails a high risk of infection. ePTFE prostheses are biostable, do not dilate, and have acceptable cell ingrowth, but they may induce stitch bleeding, increase infection risk, limit incorporation, and cause perigraft seroma formation [53]. Therefore, tailoring matrixes of vascular grafts with optimized materials, structural design, and graded stiffness are necessary to comply with the specifications of the targeted users' vessels.

In addition, tailoring the surface of vascular grafts to enable rapid and safe integration into the human body remains an ongoing challenge. Reference [54] indicates that thrombosis appears on pristine grafts more than on grafts seeded with endothelial cells. Advanced biomimetic coatings made of synthetic and non-synthetic materials must enable pre-endothelialization to ensure biological compliance and improve the overall mechanistic response of the graft surface to the host arteries. Silver [55, 56] has been applied to graft coatings to enhance their antimicrobial properties and to prevent infection in the early postsurgical stage. Similarly, sulphate-based graft coatings may also improve the long-term properties of vascular grafts by decreasing thrombogenicity and by preventing neointimal hyperplasia [57]. For vascular grafts made of ePTFE, one solution is to increase graft permeability, because the rate of tissue ingrowth is associated with graft porosity, and transmural capillary ingrowth can provide the cell source for surface endothelialization. Another strategy involves modifying the

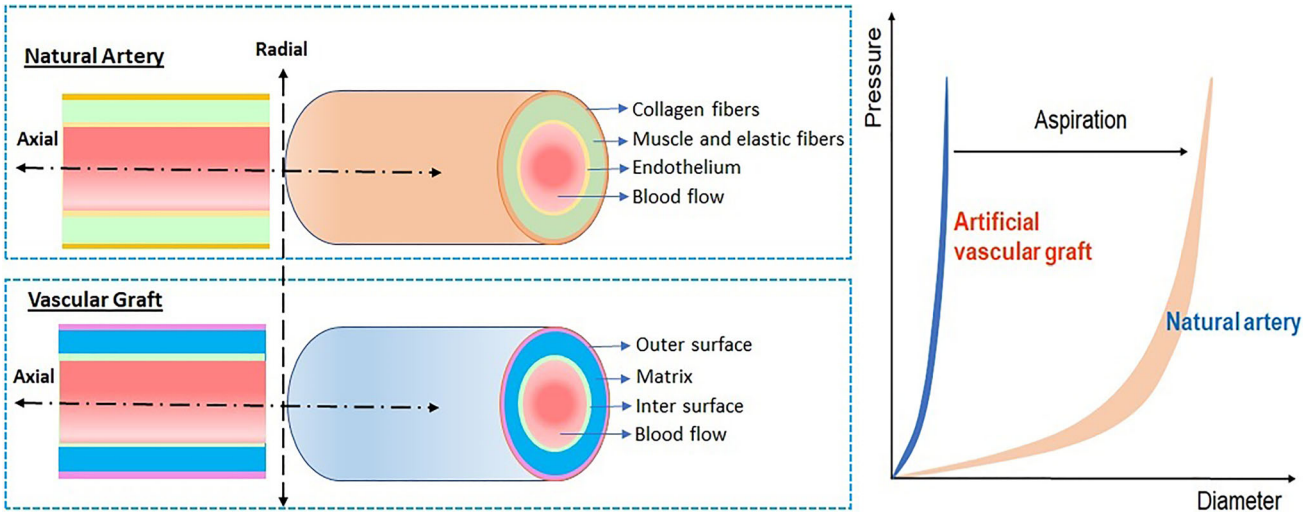

Fig. 3 The structures of a natural blood vessel (artery) and artificial implant (vascular graft), and the corresponding mismatch in their radial compliance

luminal surface of the graft. Carbon coatings have been used to increase surface electronegativity and prevent thrombus formation [58]. Diamond-like carbon (DLC) coatings possess biocompatibility [59], noncytotoxic [60], hardness [61], and wear resistance [62]. Thus, they have been used for load-bearing and non-load-bearing invasive artificial implants. DLC-coated ePTFE-based artificial vascular grafts have also ensured patency [63]. There is a need for subsequent studies to systematically investigate how to improve the matrix and surface properties of vascular grafts to overcome existing limitations.

The structural design of a vascular graft is complex. The design requirements [64] depend on the application; they include compliance, stiffness, elastic recovery, toughness, fatigue strength, buckling, and geometric parameters such as diameter and wall thickness. The current market is approaching toward conducive solutions for the development of customized vessel implants. Nonetheless, the domains of biomedical engineering and surgery have evolved over the past 20 years. Vascular grafts are now being implanted in diverse body parts, including in the arms, legs, and chest, which imposes various mechanical and structural requirements. Moreover, graft requirements are partially patient-specific and depend on sex, age, and health status. Therefore, the structural design of a graft should be created in a patient-specific manner to achieve effective long-term function. For example, the design requirements of the human aorta are location-specific. The aorta consists of an ascending section and a descending section [65]. The two sections are further subdivided into the distal and proximal ascending aorta and the proximal, mid, and distal descending aorta, which differ from each other in diameter. Furthermore, the geometry of the individual sections differs depending on age and sex. Therefore, grafts are designed with specific geometric dimensions and material properties that are appropriate for specific sections of blood vessels. Any structural incompatibility may lead to infection, toxicity, inflammations, or stroke. Hence, in the design of a composite vascular graft, mechanical, material, structural, and manufacturing aspects should be considered to achieve a high degree of customization depending on patient-specific requirements.

The Young's moduli of synthetic grafts are often higher than those of natural arteries [41, 66]. A graft made using a single material would be unlikely to rival a natural artery with respect to properties such as stiffness, elastic recovery, compliance, and porosity. Recently, the development of mechanical and biomimetic surfaces and matrix structures has revolutionized the design criteria for vascular grafts. In this study, we review progress in surface and matrix structural design, manufacturing methods, and their associated structures; in emerging composite materials for graft manufacturing; and in architectural designs, such as layered, embedded, and hybrid configurations adopted in the past few years to optimize the mechanistic behaviours of artificial grafts such that they are close to those of arteries. Figure 4 illustrates the design factors that exert a fundamental influence on the biofunctioning of composite vascular grafts.

Surface structural design of composite vascular grafts

The inner and outer surfaces of a graft directly interact with the biological environment and therefore, should be biocompatible, non-toxic, and endothelialized to ensure biocompatibility with the host. The graft surface should be able

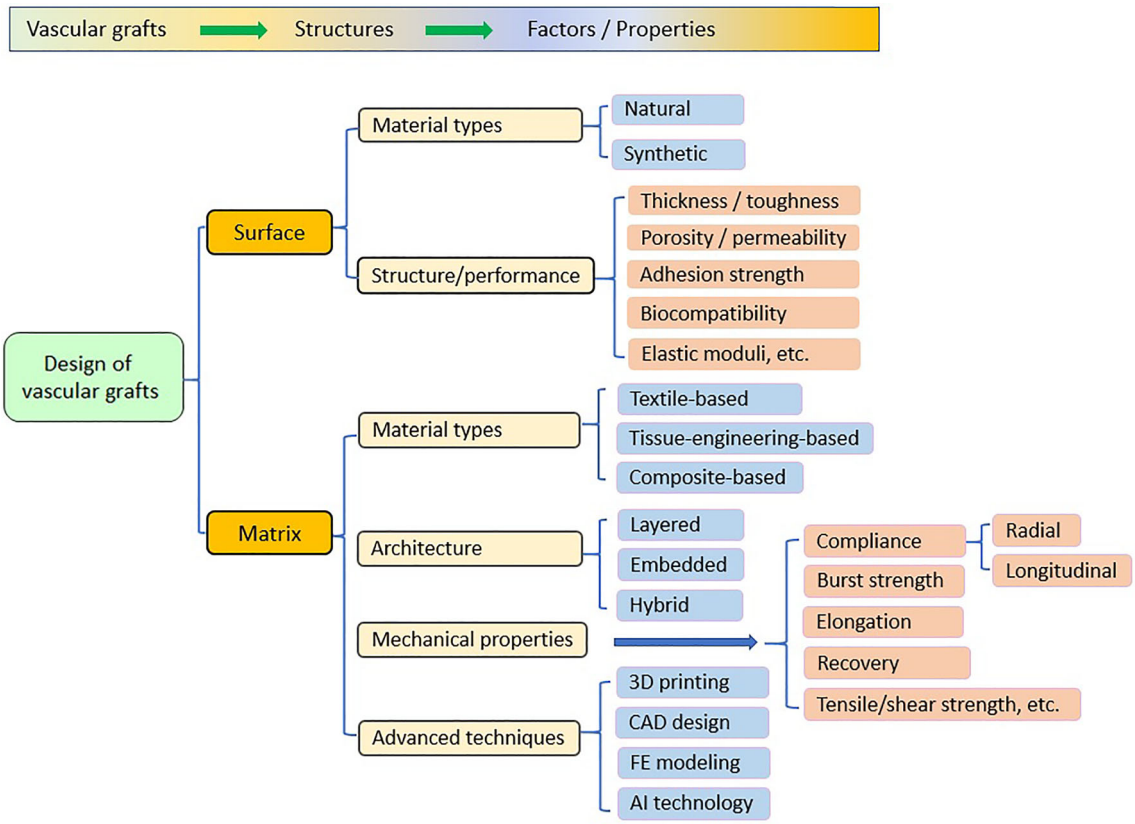

Fig. 4 Essential factors involved in the structural design of composite vascular grafts

to selectively attach to certain cells while limiting the extent of bridging with contaminants and of thrombi formation. In addition to exhibiting biomimetic functions, graft surfaces exhibit mechanical responses. Their inner surfaces are exposed to hemodynamic shear stress, which can easily cause the endothelial coating to delaminate from the matrix under high levels of stress concentrations. Accordingly, two significant aspects of the surface design of grafts can be identified, namely, biomimetic functioning and mechanical functioning.

Material design for surface structure

Blood vessels possess a layered structure (Figs. 3 and 5) comprising muscles, the basement matrix, and the endothelium in the outer-to-inner direction. The graft matrix—which is not usually biomimetic—is coated or doped with an endothelialization material to ensure biocompatibility. Thus, the endothelial characteristics of the graft surface [67], which are realized using natural or synthetic materials, produce a biomimetic environment (Table 1). Both natural and synthetic endothelialization materials have their respective merits and disadvantages. Natural materials (e.g. collagen and hyaluronan) are superior in terms of their ability to induce cell attachment and form multiple structures, but they suffer from poor mechanical properties (e.g. Young's modulus). The reverse is true for synthetic endothelialization materials. Therefore, additional chemical, physical, or biological procedures are required to boost cell attachment capabilities. There are many derivatives of natural endothelial materials. For example, collagens can be classified into 28 subtypes depending on their structures and functionalities and on their existence in different areas of the body [68]. With a combination of collagens with silver, endothelial materials can be promoted to boost antimicrobial function [69]. The selection of appropriate endothelial materials strongly depends on the matrix materials, fabrication methods, applications, and on the disease under treatment.

Depending on the manufacturing method in question, it might be possible to coat endothelial materials on the top of matrix surface or diffuse inside a graft matrix. In the case of diffused endothelial materials, a biomimetic environment is induced at a slower rate, but the risk of damage or delamination is lower. Inappropriate co-spinning of the endothelial material and graft may lead to the production of heterogeneous structure with a greater uncertainty in terms of mechanical properties. The biological efficiency of such a graft would be low because the doped material would effectively act as a defect, thus degrading the

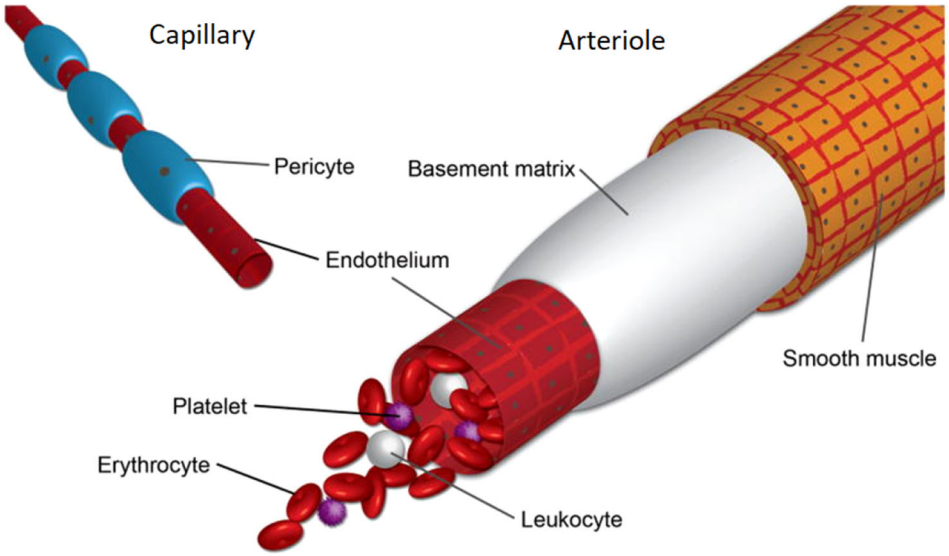

Fig. 5 Surface design as an essential part of the graft structure—endothelial material layer can be observed on the inner surface of the natural artery wrapped by the basement matrix and smooth muscle. Reproduced from [70], Copyright 2011, with permission from Elsevier Ltd

Table 1 Example list of natural and synthetic endothelial or scaffold materials

Natural materials				Synthetic materials	
Collagen	[71, 72]	Fibrin	[81, 82]	Poly(Ɛ-caprolactone) (PCL)	[92–94]
Hyaluronan (HA)	[73–76]	Silk fibroin	[83, 84]	Polyethylene glycol (PEG)	[95, 96]
Alginate	[77–79]	Peptides	[85–87]	Poly (2-hydroxyethyl methacrylate-co-methacrylic acid (pHEMA)	[97]
Matrigel	[80]	Decellularized matrix	[88–91]		

mechanical performance. Various methods have been tested to ensure the homogenous distribution of endothelial materials—for example, the continuous rotation of the graft during co-spinning. The combination of electrospinning with electrospraying has also been studied [98], wherein gelatine-based endothelial materials are electrosprayed to ensure that they are uniformly distributed throughout the graft. Scaffold-based endothelialization structures are fabricated using various techniques, such as seeding and the decellularization of natural matrixes. Figure 6 illustrates how seeding is used to boost endothelialization in scaffolds. The surface coverage increased from a fraction of the surface (Fig. 6a) to the entire surface area with a uniform coating (Fig. 6d) developed within 7 days after seeding. Similarly, according to MTT (3-(4,5-dimethylthiazol-2-yl)-2,5-diphenyltetrazolium bromide) assay results, the viability of Human Umbilical Vein Endothelial Cells (HUVECs) (Fig. 6e) and A7r5 cells (Fig. 6f) increases linearly with time. Alternatively, graft surfaces can be treated with plasma to control their surface texture, which governs their hydrophilicity or hydrophobicity, thus facilitating selective cell attachment to diffused endothelial materials and also boosting interfacial adhesion between the matrix and the endothelial coating.

Mechanical design for surface structure

Endothelialization materials can be used to not only facilitate the establishment of a biomimetic environment, but also to improve the mechanical performance of a graft in various aspects, including surface morphology [100], stiffness, compliance, porosity, and leakage resistance. Veins and arteries compliance of 9.86 and 3.59 Pa while the woven and knitted Dacron vascular grafts have demonstrated the compliance of 2.50 and 3.06 Pa, respectively [101]. Furthermore, the elastic moduli of smooth muscles, collagens, and elastin are about 0.1, 1000, and 0.6–1 MPa, respectively. By contrast, the elastic moduli of grafts made with engineering materials such as Dacron and embedding stainless steel stents are about 800–900 MPa and 190–200 GPa [101], respectively. This mismatch in elastic moduli of natural and engineered vascular materials leads to stress shielding, which degrades the mechanical responses of grafts. Hence, manufacturing techniques such as seeding, co-spinning, or coating are often used to regulate mechanical properties of graft matrixes by the integrated endothelial materials to achieve artery-like properties.

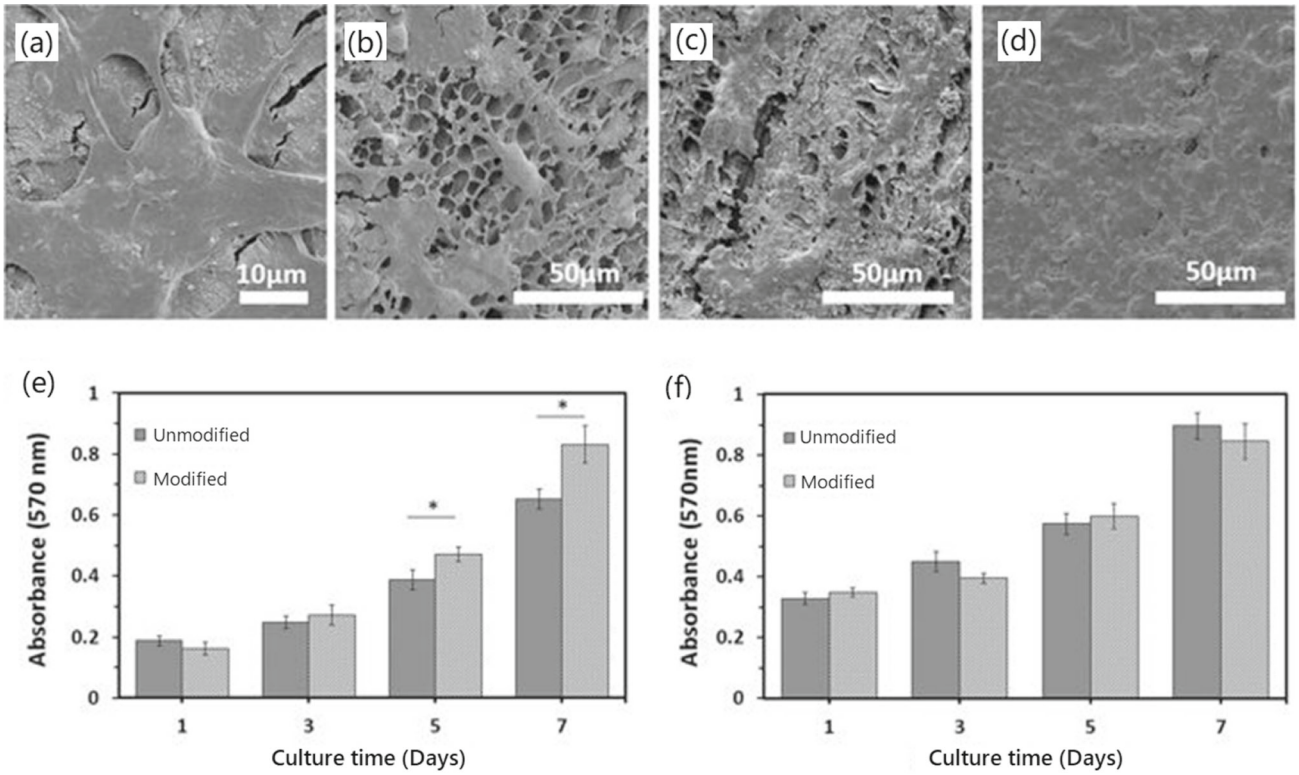

Fig. 6 Role of scaffold seeding in which cell viability increases with time in a directly proportional manner in 7 days (**a**–**d**). **e** and **f** show MTT-cell viability with HUVECs and A7r5 cells, respectively. Reproduced from [99], Copyright 2017, CC BY Springer Nature

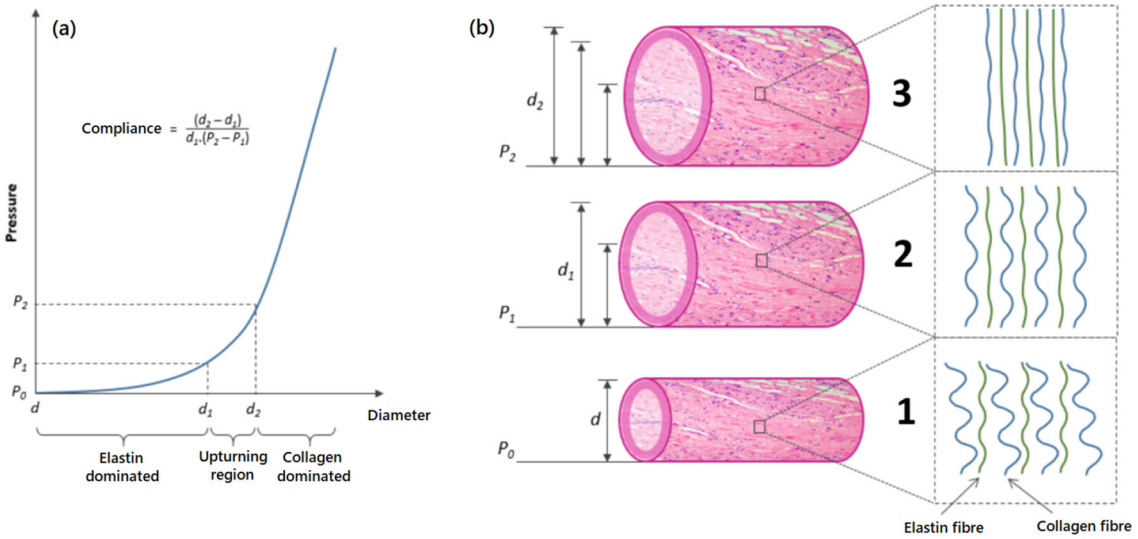

Fig. 7 **a** Role of endothelial material in the structural performance of the artery and **b** mechanistic behaviour of endothelial materials in response of increasing pressure. Reproduced from [101], Copyright 2015, CC BY Multidisciplinary Digital Publishing Institute, Switzerland

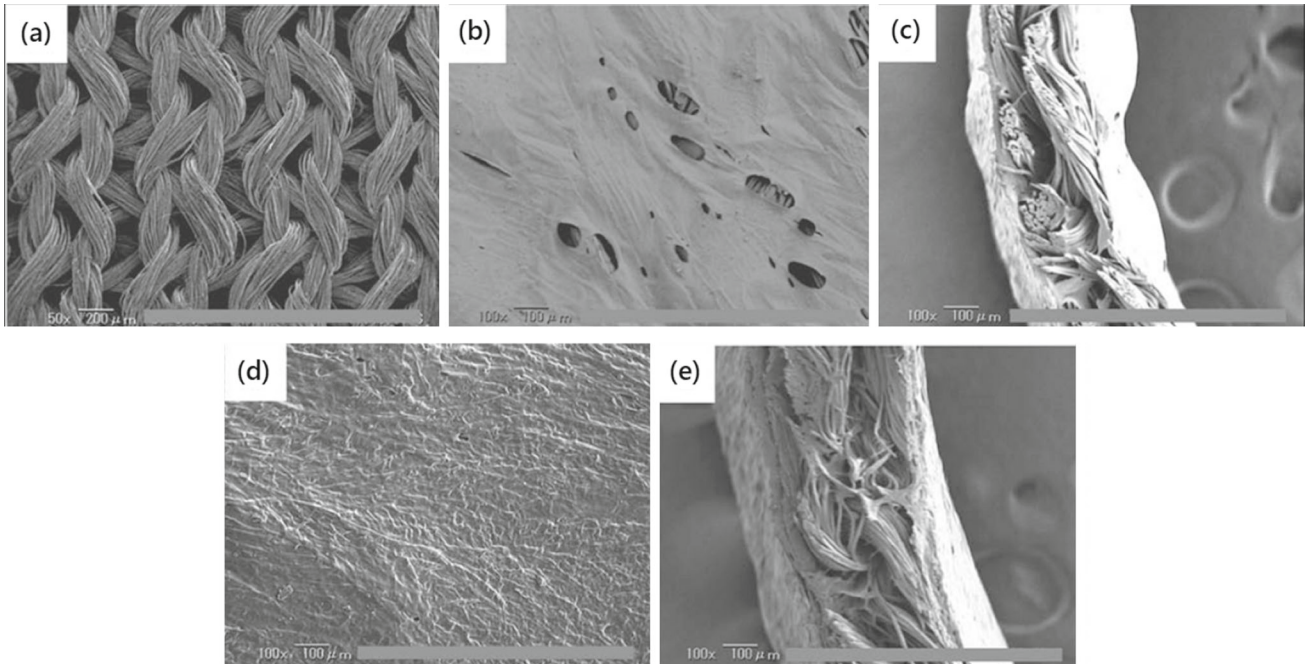

Fig. 8 Scanning electron micrographs of silk fibroin grafts **a** without coating, single layer in the **b** plane view, and **c** cross-sectional view; as well as double-coated **d** in the plane view and **e** in the cross-sectional view. Reproduced from [106], Copyright 2013, with permission from John Wiley & Sons

Figure 7 illustrates the roles played by elastin and collagen in the structural performance of an artery. A hierarchical structure with ordered layers of elastin and collagen fibres is evident. Figure 7a shows the compliance curve, in which the artery diameter increases nonlinearly with pressure. The role of elastin fibres is dominant in the normal pressure range, that is, P_0 to P_1, and both elastin and collagen fibres exhibit spiral structures in the case of a normal artery diameter d, as illustrated in Fig. 7b-1. Once the pressure increases from the low range to the medium range (P_1 to P_2), the elastin and collagen fibres tend to flatten, thus increasing the arterial diameter from d to d_1 in response to the change in blood pressure, as illustrated in Fig. 7b-2. As noted, the Young's moduli of elastin and collagen are 0.6–1 and 1000 MPa, respectively. Therefore, the role of elastin becomes limited, and collagen primarily governs the further expansion of the arterial diameter from d_1 to d_2 as the pressure increases continuously beyond P_2, as illustrated in Figs. 7a and 7b. The schematics depicted in Figs. 7b-1–7b-3 illustrate the elastic response of endothelial materials. The structures of these materials transition from a spiral shape to a flattened shape within their elastic limits in response to changes in pressure. This natural mechanism has been mimicked in various bioengineering studies. For example, collagen-coated, woven Dacron was successfully used to achieve a radial expansion of up to (11 ± 4) % in the case of a graft with a diameter of 26 mm [100] without localized aneurysmal dilatation. Notably, endothelial materials are hampered by structural limitations in terms of their elasticity, and excessive blood pressure may push such materials beyond their elastic limits, leading to rupture or delamination. Therefore, in addition to the material configurations of such materials, their geometric textures can be engineered for the same purpose; for example, several graft composites are produced with plane, wavy, or patterned textures.

Dimensional design for surface structure

Dimensional aspects include porosity, thickness, and coverage area. Porosity control is an essential characteristic of endothelial materials [102, 103]. Highly porous grafts are more susceptible to blood leakage, thus requiring more healing time. In this context, endothelial materials can be used to reduce porosity, especially in the case of textile-based grafts, and to regulate biological functioning. Crosslinked bovine collagen can be used to reduce the porosity of knitted, double-velour Dacron grafts from 1400 to 0 cc/(min·cm^2) [104]. Similarly, a collagen succinylation can be applied to reduce water leakage and homeostatic time of e-PTFE grafts from (169.9 ± 38.5) mL/min to (34.5 ± 29.9) mL/min and (34.2 ± 11.5) min to (4.5 ± 2.5) min, respectively [105]. Figure 8 depicts representative images of knitted grafts without coating, with a single coating, and with a double coating of a silk fibroin material. As illustrated in the figure, porosity, which causes blood leakage, decreases considerably after the knitted graft is coated with an endothelial material. The capacities

of various endothelialization materials to reduce porosity differ.

Endothelial materials are usually soft and may undergo structural changes, such as the delamination of their coating or an increased porosity when subjected to high blood pressure and turbulence. Textile-based vascular grafts have a potential to lower the porosity, and the extent of reducing porosity increases with increasing number of fabric layers. The coatings are usually prepared using the dip-coating technique, and occasionally, additional pressure is applied to the fluid to enhance the penetration of the endothelial material. Depending on the level of porosity—which is higher in the case of knitted structures and lower in case of woven structures—a single coating or multiple coats may be applied either on the inner surface of the graft or on both the internal and external surfaces to fulfil the design requirements. Along with single- or dual-side coatings, an increase in the number or density of the fabric layers not only reduces porosity but also improves the mechanical properties of the graft. Figure 9 depicts the morphology and mechanical properties of PU vascular grafts reinforced with weft-knitted tubular fabric. The plane surface and the cross section of this fabric exhibit overly high porosities. Hence, as the number of fabric layers increases, the tensile strength increases to five times the original value, and the overall porosity reduces at the same time.

Figure 10 illustrates the effect of surface topography on graft stiffness. The surface roughness and porosity of the knitted surface change significantly after it is coated with endothelial materials. In addition, the stiffness of the surface is altered by fabrication method, such as knitting or weaving. The uncoated knitted scaffold has a stiffness of (9.1 ± 2.38) N/mm, which can be increased to approximately (16.8 ± 4.88) N/mm when it is manufactured from the same material by using a weaving technique. Because the stiffness of the endothelial materials is lower, by coating them onto knitted scaffolds, the overall stiffness of the knitted scaffold can be reduced to approximately (5.7 ± 0.48) N/mm [108]. Hence, a judicious selection of endothelial materials is essential to satisfy the requirements for the given application, and grafts may sometimes require more than one coating layer or an additional (e.g. ultraviolet [UV]) treatment for enhanced networking in order to improve their surface topography. For example, in one study, the platelet accumulation ratio increased by almost 100% after correcting for activity diffusing into the wall during 1–4 h reperfusion when single-sealing with a collagen coating was replaced by double-sealing [109]. In another study, when a collagen-coated graft was used, (11.9 ± 5.2) days were required to perform chest drainage, whereas the same task was completed in (7.9 ± 4.6) days when a gelatin-coated graft was used [110].

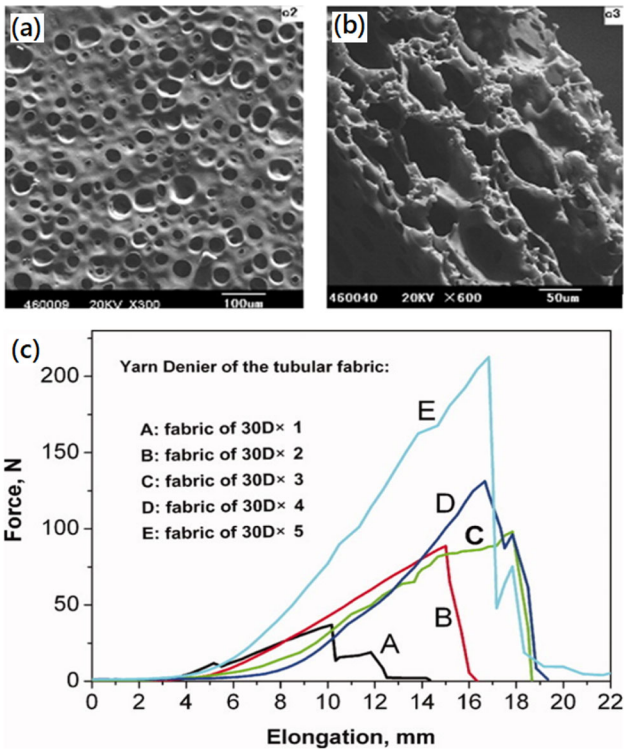

Fig. 9 Morphologies in the **a** plane view, **b** cross-sectional view, and **c** the tensile strength of polyurethane vascular grafts reinforced by weft-knitted, tubular fabric. Reproduced from [107], Copyright 2010, with permission from Wiley

Matrix design of composite vascular grafts

In Surface structural design of composite vascular grafts, we discussed the surface design of vascular graft composites with the aim of achieving compliance levels similar to those of blood vessels [111]. When considering this goal, matrix structural design is an equally important consideration. Typically, the radial compliance of an artery is proximately 7.4% mmHg × 10^{-2}, whereas that of a polyester-based woven graft is approximately 1.9% mmHg × 10^{-2} [101]. A wide range of materials have been investigated in the pursuit of biomimetic compliance, but all of them have certain limitations. The literature pertaining to structural design, distinguished by whether it focuses on radial or longitudinal (axial) designs, is reviewed in detail in this section.

Radial matrix design

Natural arteries can radially expand to a certain extent to accommodate hemodynamic turbulence beyond the normal limits of cardiac cycles. Arteries absorb energy during expansion and return to their original diameter after the passage of turbulence by releasing the stored energy. Hence, to achieve graft performance similar to that of natural arteries, it is important to ensure that vascular grafts possess significant

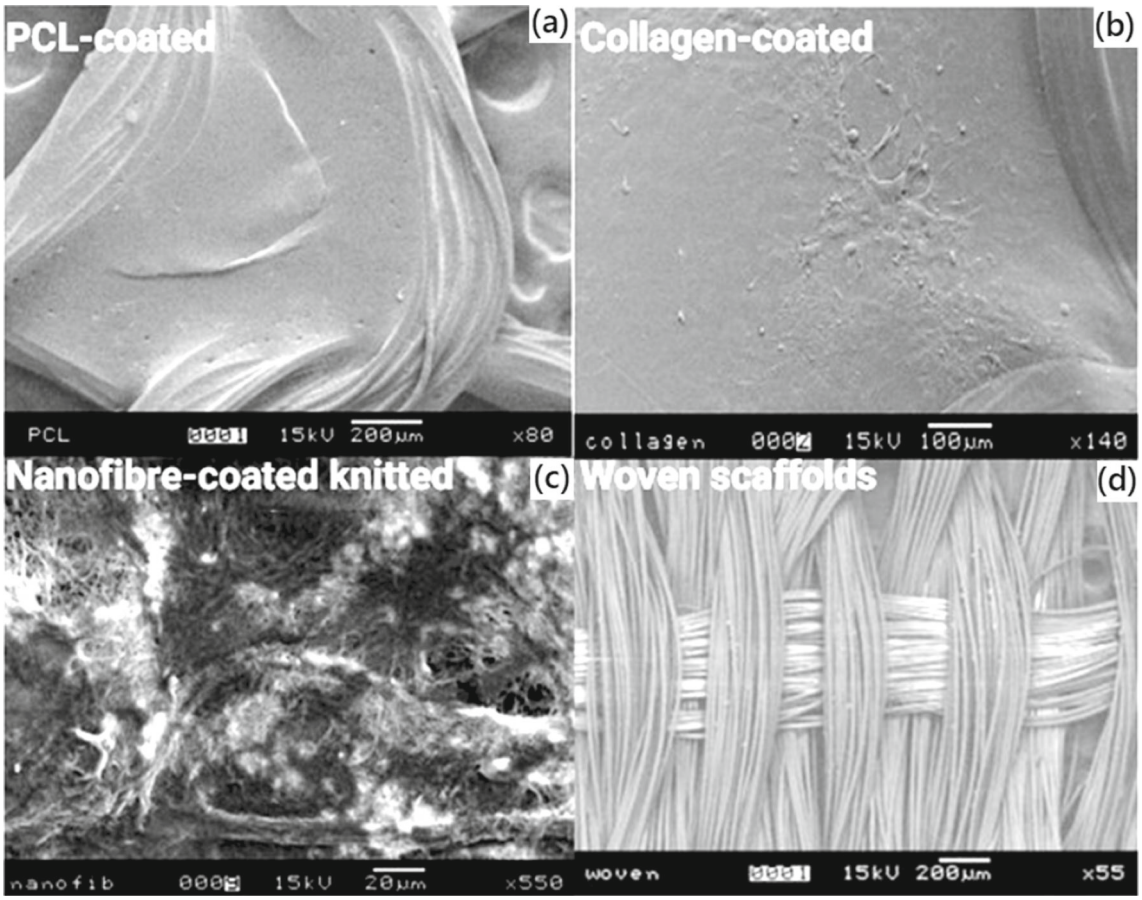

Fig. 10 Scanning electron micrographs of the knitted scaffolds coated with **a** PCL—poly(Ɛ-caprolactone), **b** collagen, and **c** nanofibers; and **d** woven scaffold without coating. The stiffness of the bare knitted scaffold changes from (9.1 ± 2.38) N/mm to about (4.3 ± 0.91) N/mm for PCL-coated, about (5.7 ± 0.48) N/mm for collagen-coated, about (5.8 ± 0.70) N/mm for nanofibers-coated, and about (16.8 ± 4.88) N/mm for woven scaffolds without coating. Reproduced from [108], Copyright 2007, with permission from IOP Publishing Ltd

expandability and elastic recovery. Recently, research focus has shifted to structural design to improve graft compliance. Figure 11 illustrates techniques used to enhance the radial compliance of graft composites. A triple-layer vascular grafts [112] composed of a silk filament, polyacrylamide (PAM), and thermoplastic polyurethane (TPU) were developed. It has the capability to radially expand TPU/PAM hybrid to provide sufficient strain for the graft to stretch radially outwards for resisting increases in blood pressure. Once the blood pressure decreases, the fibres recoil to their original position. This gives the graft material good elastic recovery and fatigue strength and, by extension, a long service life.

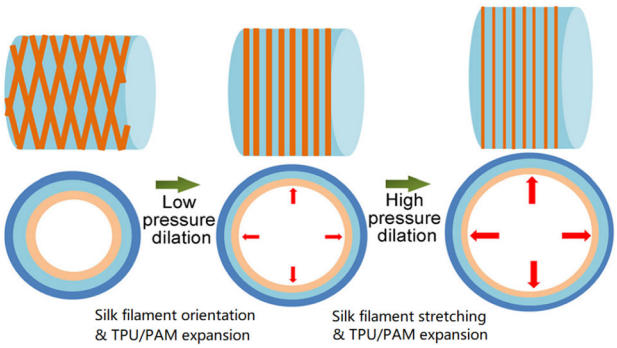

Fig. 11 Silk, polyacrylamide (PAM), and thermoplastic polyurethane (TPU)-based structural design that allows the graft composite to expand under high-pressure blood flow. Reproduced from [112], Copyright 2019, with permission from Elsevier Ltd

Longitudinal (axial) matrix design

Longitudinal compliance is the key to safely and sustainably joining a vascular graft composite with natural arteries, and it also minimizes damping across the joint. The structural and material properties at the suture connections must be well matched to prevent intimal hyperplasia. A mismatch in compliance leads to the weakening of graft walls due to impedance or vibration and to a loss of endothelial cells. Therefore, hybrid designs that offer both radial and longitudinal compliance in a single graft are currently being

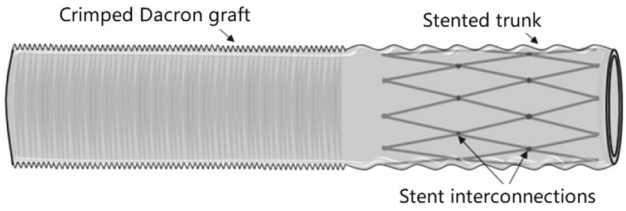

Fig. 12 A graft composite with a hybrid design to meet radial compliance and interconnection requirements. Reproduced from [36], Copyright 2017, CC BY AIMS Press

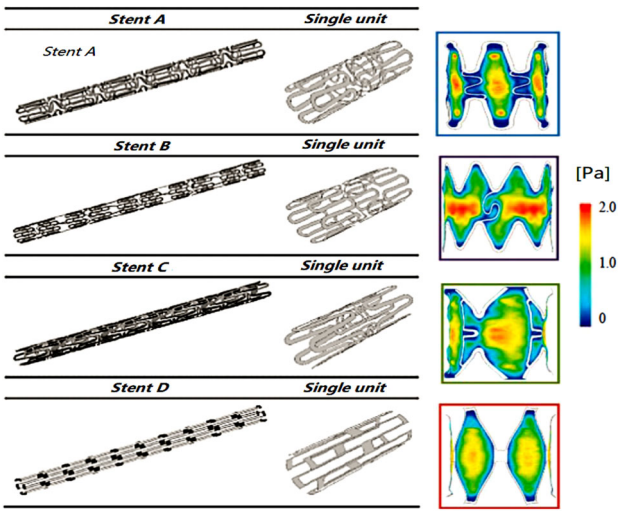

Fig. 13 Role of computational studies in optimising the structural design of stent-graft hybrids. Reproduced from [133], Copyright 2007, with permission from Elsevier Ltd

developed. Figure 12 displays a graft with a hybrid structure, in which the central body is fabricated using crimped polyester to provide extended elasticity, whereas the ends are uncrimped and embedded with Z-shaped rings that act as a stent trunk and provide safe interconnections with the arteries and strong compatibility with sutures. Additional information on hybrid designs and compliance can be found in Refs. [113–117].

Advanced matrix design

The process of improving graft design relies on an intensive cycle of design, prototyping, redesign, and optimization. Computational methods have greatly aided the design of next-generation grafts that satisfy specific requirements in customized applications.

Figure 13 depicts the process of the computer-aided design of stent-graft hybrids customized to fulfil mechanical requirements, such as high stiffness, compliance, or pressure distributions. The figure shows a comparative study of four types of stents, each having different mechanical structures. Magnified views of the stents are depicted in their corresponding single boxes. The different mechanical structures are then analysed using standard models, such as Poiseuille's law—which defines a relationship between blood flow viscosity and the internal artery/graft radius. Although the stents undergo similar levels of shear stress, their shear stress distributions differ under the same testing conditions owing to differences in their mechanical structure. Similarly, computational studies have revealed not only the radial compliance but also the hemodynamic response throughout grafts in either the radial or non-radial direction. Figure 14 illustrates the blood-velocity contours and the corresponding shear stresses in the systolic and diastolic cycles at different positions along the axial direction of the graft. The velocity of blood flow in a systolic pulse is higher than that in a diastolic pulse [118].

Computer-aided design packages and finite element (FE) modelling help designers quantitatively and qualitatively visualize application-specific factors, such as stress–strain distributions, stress concentrations, and shear stresses. These factors are crucial for designing and redesigning vascular grafts until an optimized solution is achieved. Detailed information on computational studies related to graft design, hemodynamic responses, and shear stress distributions can be found in Refs. [119–132].

Structural design of vascular grafts for optimising mechanical performance

To improve and optimise mechanical properties, the structures of vascular grafts have been designed and fabricated with various modalities (scaffold-based, non-scaffold-based, knitted, and woven materials with layered, embedded, and hybrid structures), which are summarized in Table 2 along with their corresponding sub-classifications, followed by the details of each structure and representative examples.

Textile-based structures

Medical, textile-based grafts possess excellent mechanical and biological features and are the subject of active research. Textile-based grafts can be prepared using weaving or knitting techniques, both of which lead to various types of structures that exhibit different mechanical properties. Figure 15a depicts the structures of woven grafts. The directions of the warp and weft filaments can be patterned to prepare various types of woven structures, such as plain weave, twill weave, or satin weave. In recent years, bilayer and triple-layer woven structures have been patented [134–138] or scientifically investigated [139, 140] because of their hypothesized advantages in mechanical functioning. Structures woven with a filament over-under pattern of

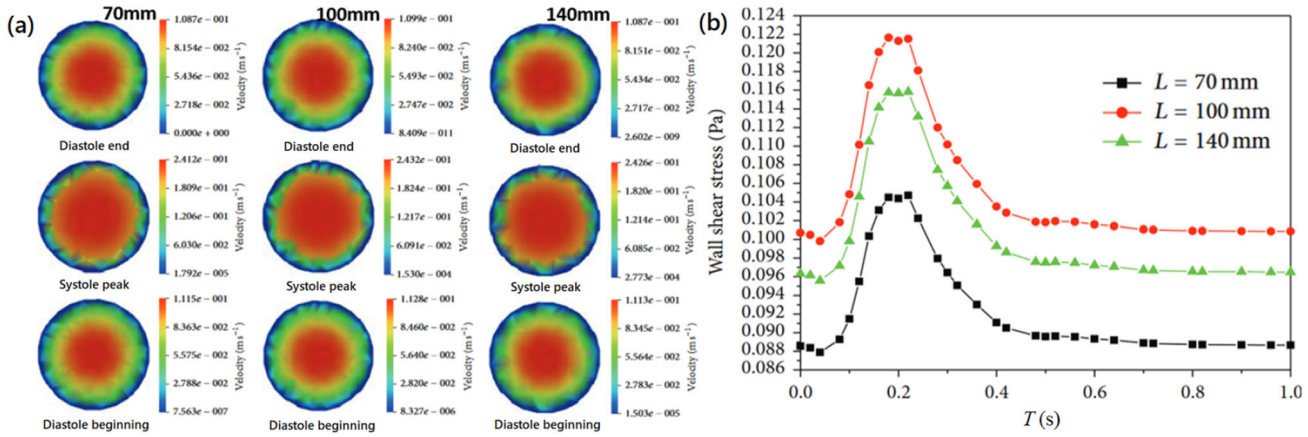

Fig. 14 **a** Velocity contours at different instances of the hemodynamic cycle and their corresponding **b** shear stress variations analysed at different portions of the graft along the longitudinal direction in order to understand the graft response to mechanical pressures posed by the blood circulation. Reproduced from [118], Copyright 2015, CC BY Hindawi Ltd

warp and weft possess minimal porosity, low creep, and a good surface finish. The interlayer or intralayer structural arrangement of the warp and weft filaments and the weaving parameters [140, 141] significantly affect the fracture mechanics of the resulting grafts. Hence, the warp and weft patterns are key to tuning the mechanical and physical properties of grafts. The properties of knitted grafts also vary with the architecture of the interlocking yarn loops, resulting in diverse structures including jersey, locknit, reverse locknit [142], weft knit, or warp knit structures, as illustrated in Fig. 15b. Grafts with knitted structures typically exhibit higher radial expansibility. However, additional coatings are required to control their porosity. Figure 16 depicts the stress–strain curves of knitted and woven Teflon and Dacron strips and grafts in both the radial and axial directions. For both flat-strip and tubular grafts, the knitted structures have higher levels of radial compliance. Moreover, the axial compliance of knitted strips is higher than that of woven strips, but this difference decreases within three weeks of implantation. In addition to mechanical properties, physical properties are greatly influenced by the manufacturing technique. For example, woven structures are microporous, stiff, difficult to suture, but require minimal preclotting. By contrast, knitted structures are macroporous, relatively comfortable and are easy to suture, but they require significant preclotting.

Table 2 Classification of graft structures based on manufacturing methods, architectures, and their sub-categories

Classification on the basis of manufacturing methods		
Method	Sub-classification	References
Textile-based structures	Weaving-based technique	[134–141]
	Knitting-based technique	[142, 143]
Tissue–engineering–based structures	Non–scaffold–based structures	[144–149]
	Scaffold-based structures	[150–155]
Classification on the basis of architectures		
Architecture	Sub-classification	References
Embedded structures	Mesh or fabric embedded grafts	[156, 157]
Layered structures	Structures made of monolayer, bilayers, triple layers, and multiple layers	[112, 158–164]
Hybrid structures	Structural and materials combinations	[165–172]

Tissue engineering-based structures

Graft structures based on tissue engineering can be categorized into non-scaffold-based and scaffold-based grafts. Figure 17 depicts the workflow for preparing tissue-engineering-based (scaffold- and non-scaffold-based) grafts by diffusing endothelial cells into the graft using decellularized natural-matrix technique. First, tissues are obtained from patients, and the cells are processed by following the isolation and expansion protocols illustrated in Figs. 17a and 17b. Then, the cells are further diffused into scaffold-based or non-scaffold-based grafts, as depicted in Fig. 17c. The simplest method involves electrospinning a porous graft that is subsequently combined with the cells. In another strategy, porous grafts can be prepared by freeze drying [144–146], followed by cell diffusion. In addition, non-scaffold-based grafts can be prepared using the decellularized natural matrix technique. In this approach, the cells are mixed with a gel,

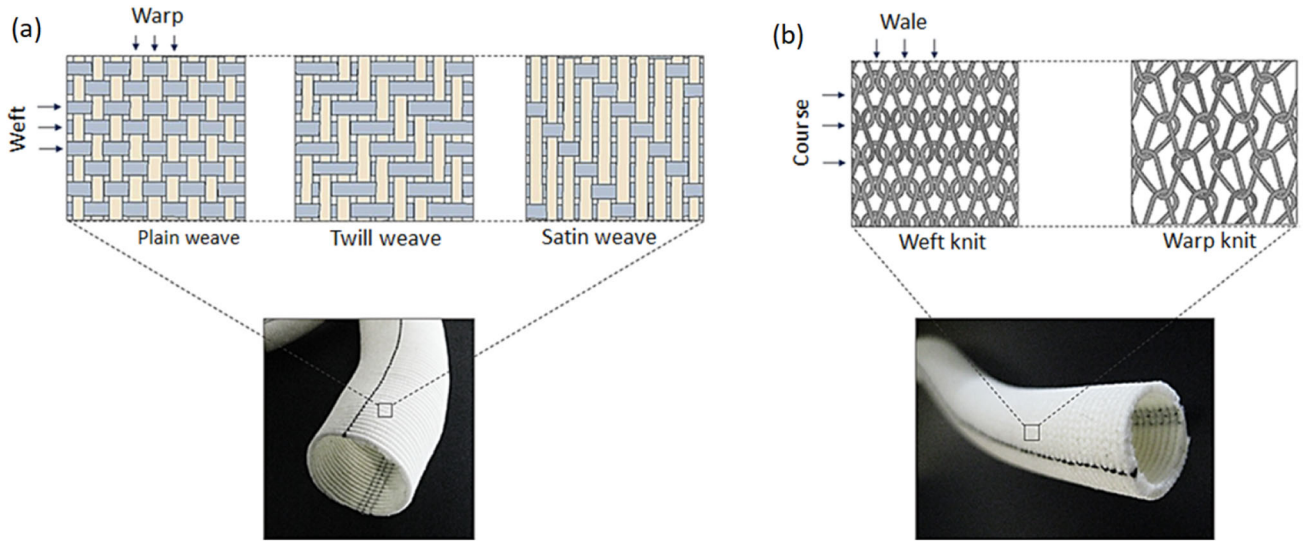

Fig. 15 Grafts with different structures are made with **a** weaving and **b** knitting technologies. Reproduced from [101], Copyright 2015, CC BY Multidisciplinary Digital Publishing Institute, Switzerland

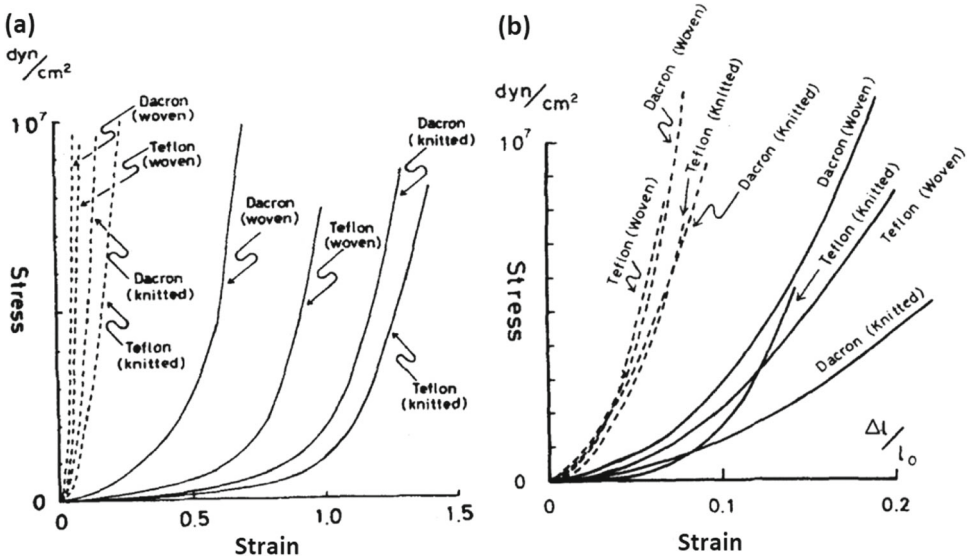

Fig. 16 Stress–strain curves of **a** strips and **b** grafts made of Teflon and Dacron with knitted and woven structures. The solid and dotted lines represent axial and radial directions, respectively. Reproduced from [143], Copyright 1979, with permission from Elsevier Ltd

which is further mould-cast to form a vessel-like shape. Similarly, there exist decellularized grafts, in which vascular or non-vascular tissues are decellularized with nucleases, thermolysin, or phospholipase enzymes and detergents, such as octylglucoside, or sodium-based chemicals, such as sodium dodecyl sulphate or sodium deoxycholate by using combinations of mechanical and physical methods followed by cell diffusion. Once the cells are diffused, dynamic maturation (Fig. 17d) is performed before implantation (Fig. 17e). The scaffold- and non-scaffold-based methods are detailed in the following subsections.

Non-scaffold-based structures

Non-scaffold-based vascular grafts are generally fabricated by means of mould casting, micro-tissue aggregation, and bioprinting methods. The manufacturing techniques and structures of non-scaffold-based grafts are depicted in Fig. 18. Cell-sheet-based grafts—comprising an adhesive and confluent layer of cells—are formed and wrapped around a mandrel, followed by dynamic maturation, to form a graft shape, as shown in Fig. 18a. Tubular cell grafts are produced by pouring cell-suspension-containing droplets into a mould, where they adopt a tubular shape owing to the in situ amalgamation of cells, as illustrated in Fig. 18b. Bioprinted spheroid cell grafts (Fig. 18c) are especially versatile and have been continually developed in recent research. In this technique,

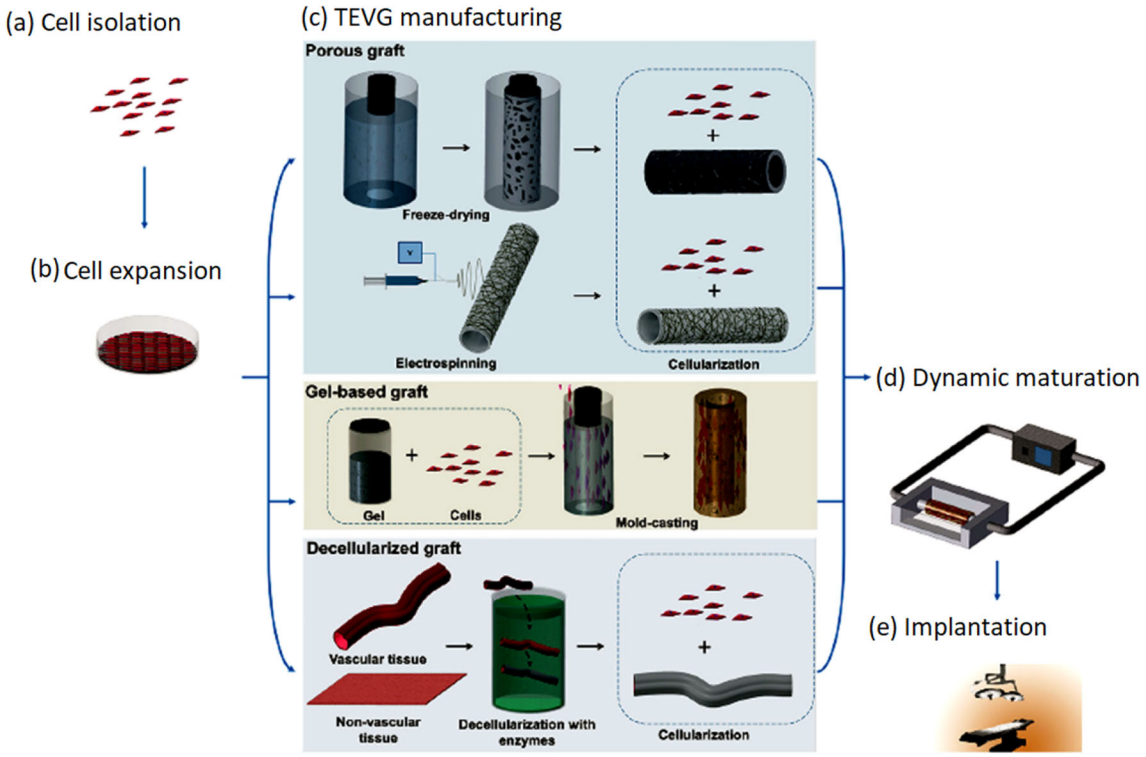

Fig. 17 Preparation of scaffold and non-scaffold grafts with decellularized natural matrices. The patients' tissues are processed for **a** cells isolation and **b** cells expansion and **c** are diffused in grafts prepared and passed through **d** dynamic maturation before **e** implantation. Reproduced from [147], Copyright 2018, CC BY Frontiers Media SA

spheroids of a cell suspension are deposited on a support material and merged to form a graft, after which the support material is removed. Details on non-scaffold-based vascular grafts can be found in [148, 149].

Scaffold-based structures

Scaffold-based graft structures are typically produced by means of electrospinning [150–153]. The electrospinning process produces polymer filaments of specified diameters that are stacked layer-wise to create a thick scaffold. These grafts are usually electrospun using synthetic polymers such as polylactic acid, PCL, polyglycolic acid (PGA), ploy-L-lactide (PLLA), poly(ester urethane)urea (PEUU), poly(4-hydroxybutyrate) (P4HB), poly(glycerol sebacate) (PGS), PU, or natural biomaterials such as fibrin, silk fibroin, collagen, elastin, chitosan, and gelatin [154]. The popularity of electrospinning can be attributed to its greater technical flexibility, which allows for the manufacture of grafts from either a single material or by co-spinning two or more materials in specified proportions. Moreover, the flexibility of co-spinning wide range of materials also allows for the co-spinning of endothelial-materials graft manufacture, thus eliminating the requirement of pre-surgery graft endothelialization. Figure 19 depicts the electrospinning method for graft manufacturing as well as the plantar and cross-sectional structures, compositions, and mechanical properties of electrospun grafts [155]. Figure 19a illustrates the co-spinning of grafts composed of PCL, polydioxanone (PDS), and a PCL/PDS hybrid. Figure 19b shows cross-sectional and planar structural views of the PCL, PDS, and PCL/PDS grafts. The filaments of the three types of polymers differ notably in terms of their diameters. Additionally, the PCL and PDS filaments in a hybrid graft are highlighted in a colour-graded fluorescence image. The structural effects on the physical and mechanical properties of the filaments are illustrated in Figs. 19c–19h. The larger filament diameter of PCL increases the graft porosity when it is prepared in the form of a scaffold. PDS is less porous, whereas the hybrid material has an intermediate porosity. Likewise, PCL is hydrophobic and PDS is hydrophilic, whereas the PCL/PDS hybrid has intermediate hydrophobicity. The other properties of PCL/PDS hybrid grafts—such as the Young's modulus, tensile strength, and elongation—lie between those of their pure counterparts. Details pertaining to scaffold-based vascular grafts can be found in Refs. [150–155].

Embedded structures

Most grafts are made from soft polymers and may therefore not satisfy the stiffness and rigidity requirements of

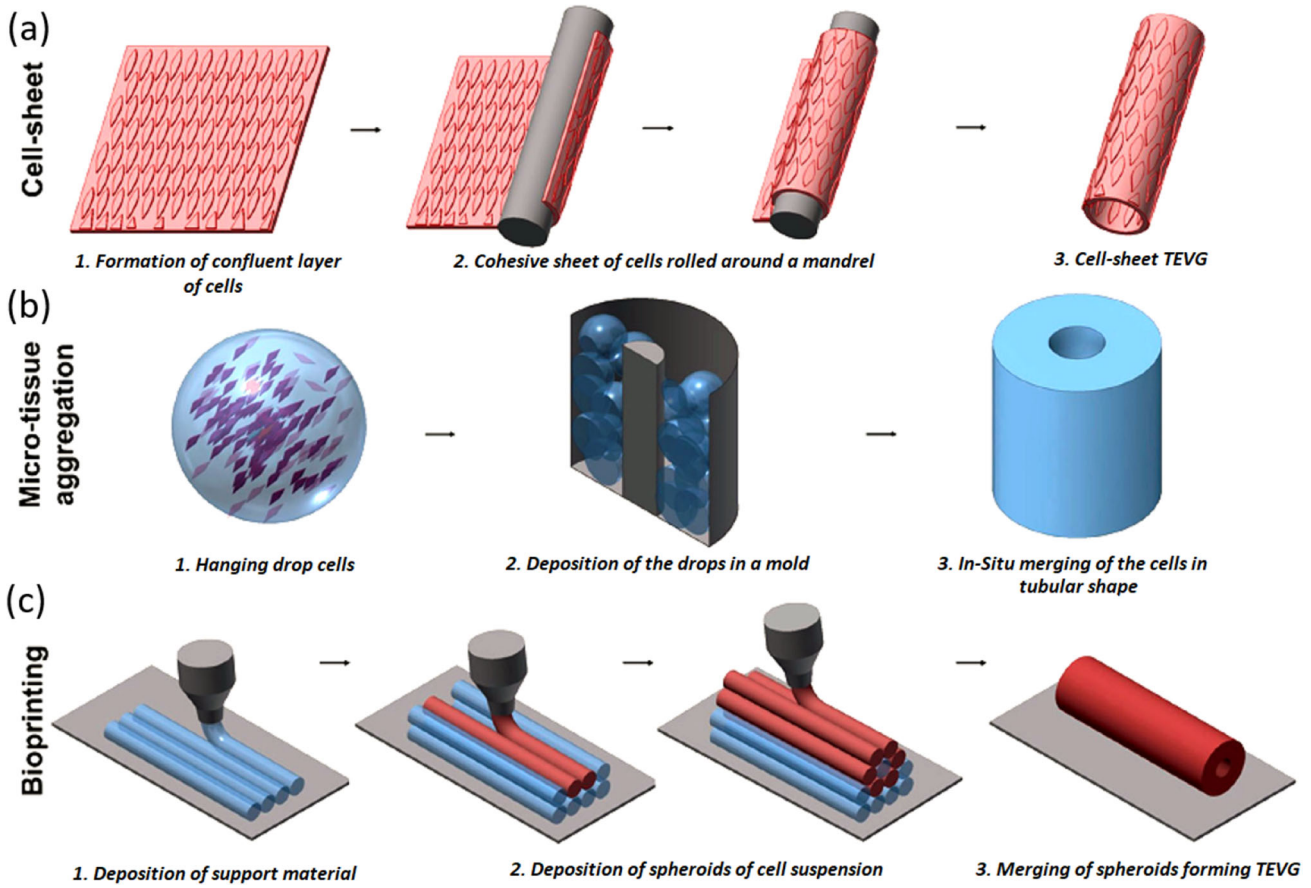

Fig. 18 Non-scaffold-based vascular grafts are made with **a** cell-sheet, **b** micro-tissue aggregation, and **c** bioprinting. Reproduced from [147], Copyright 2018, CC BY Frontiers Media SA

specific graft applications. In such cases, additional parts that have superior mechanical properties, such as stents, are embedded into the grafts. Figure 20a depicts an idealized, three-dimensional (3D) wire mesh prepared by knitting. Such structures are either encapsulated in the graft to provide structural support, as illustrated in Fig. 20b, or embedded in the graft wall to increase the overall strength, as depicted in Fig. 20c. Figure 21a presents a schematic of a composite graft composed of PU and embedded with tubular fabric. The corresponding radial strengths are illustrated in Fig. 21b. PU has a low radial strength of about 8 N, whereas the tubular fabric is approximately fivefold stronger at about 45 N. The tubular-fabric-embedded PU has a radial strength of about 38 N. Thus, the radial strength of the PU graft is increased by 375% owing to the embedded tubular fabric.

Layered structures

The first vascular grafts were monolayer grafts and were usually prepared by means of extraction. However, bi- and triple-layer configurations with improved mechanical performance have quickly replaced monolayer grafts. Bi- or triple-layer grafts can be made from textile- or tissue-engineering-based structures or their hybrids. Furthermore, multilayer grafts are designed using the same principles to enhance structural durability.

Bi-layer structures

Bi-layer structures [158] are designed to achieve subject- and application-specific mechanical properties of vascular grafts. The two layers may vary in terms of material, geometry, structure, compositions, orientations, or manufacturing method to achieve a desired level of compliance, tensile strength, and elastic recovery. Figure 22 depicts a bi-layer graft prepared by means of electrospinning. The inner layer is composed of aligned PCL/collagen fibres, whereas the outer layer is composed of PCL/silica fibres. Generally, PCL has a tensile strength of 10–16 MPa, whereas micro-structured silica fibres may have a tensile strength of about 5,000 MPa [159]. Thus, the addition of silica fibres increases the overall tensile strength of the graft. Figure 23 presents the corresponding mechanical properties of the aforementioned

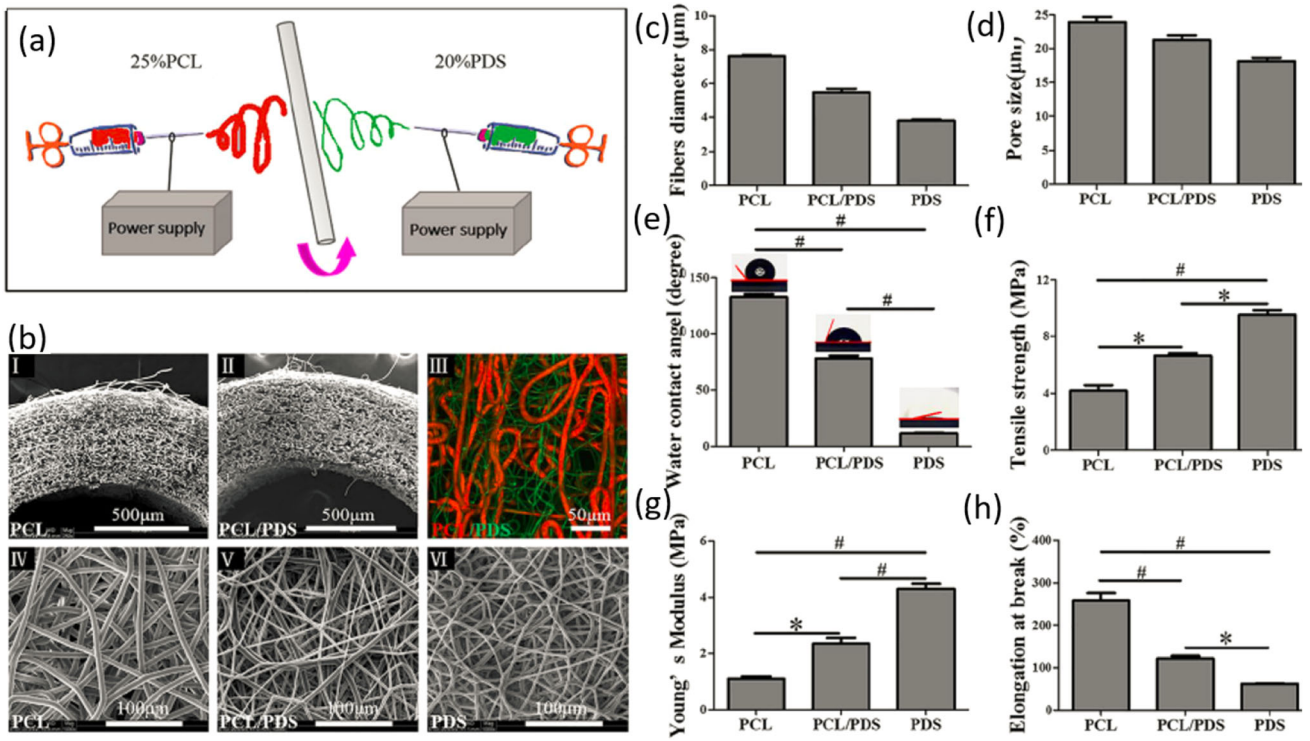

Fig. 19 Scaffold-based grafts made with the **a** electrospinning of PCL, PDS, and their combination. The scaffold structures are observed in **b** scanning electron micrographs and **c**–**h** present their physical and mechanical properties. Reproduced from [155], Copyright 2017, CC BY Springer Nature

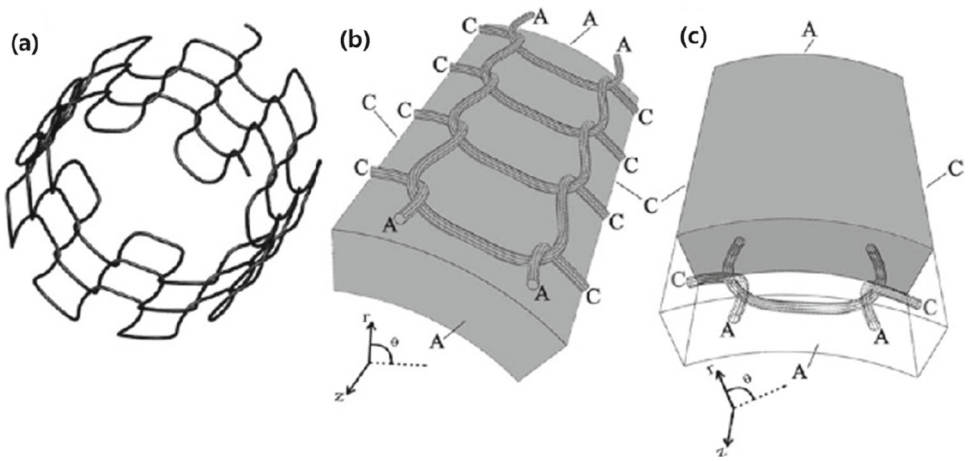

Fig. 20 Graft with embedded structures: **a** mesh structure/stent, **b** mesh structure encapsulating polymer layers, and **c** mesh structure embedded in polymer layers. Labels **A** and **C** represent surfaces that obtained axial and circumferential boundary conditions, respectively. Reproduced from [156], Copyright 2010, with permission from Springer Nature

bi-layer graft. The ultimate tensile strength and Young's modulus increase two to three times in both the axial and radial directions after the addition of silica. However, because silica is brittle, its addition reduces the elongation capacity of the graft by up to 50%, as can be inferred from the corresponding axial and radial stress–strain curves depicted in Fig. 23a. Silica fibres can cause a threefold improvement in suture retention strength along the axial direction, as shown in Fig. 23b.

Triple-layer structures

Combining multiple materials is not always beneficial in every aspect. The advantages of doing so are generally accompanied by drawbacks. As detailed in the preceding section, although silica can improve the radial and axial tensile strength of grafts, it reduces their elongation capacity. Polymers intrinsically exhibit plasticity with aging. Therefore, triple-layer grafts are manufactured using the same raw material either with alternative manufacturing techniques (such as electrospinning, electrospraying, or their

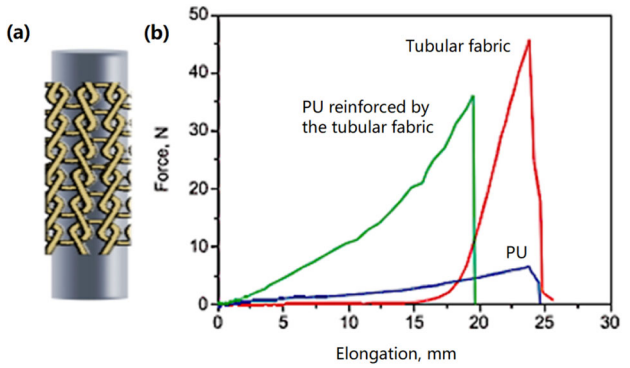

Fig. 21 **a** Illustration of a graft with a reinforced structure and their corresponding **b** radial strength. Reproduced from [157], Copyright 2009, CC BY Institute of Biopolymers and Chemical Fibres

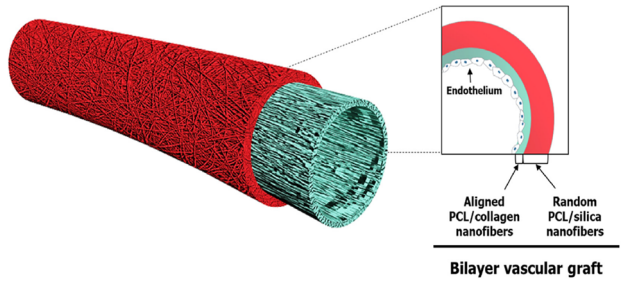

Fig. 22 A bilayer graft made by the electrospinning of an inner layer with PCL/collagen fibres and an outer layer of PCL/silica fibres. Reproduced from [160], Copyright 2019, CC BY Elsevier Ltd

combinations—which alter the produce behaviour) or in different physical forms [112, 161, 162], such as textile-based polyesters or additively manufactured forms of polyester. These trends are emerging in recent research with the goal of improving graft performance and reducing graft plasticity. Thus, appropriate material selection and an optimization of the trade-off between various material properties strongly depend on the design criteria of specific applications. Such requirements have been spurring advances in minimizing the structural deficiencies of vascular grafts. Natural arteries expand and retract while absorbing and releasing energy. In practice, engineering materials are not perfectly elastic but are subject to time-dependent plasticity due to the fatigue imposed by the functioning of the graft under hemodynamic pulsations. Figure 24 presents the micrographs of a triple-layer vascular graft developed in [112] designed to maximize elastic recovery. This graft is composed of one layer of silk, TPU, and PAM. The silk layer was braided into a tube that was immersed in a poly(dimethylsiloxane) (PDMS) mould to form a PAM tube, which was further electrospun with TPU to form a triple-layer structure. Figure 24a presents a cross-sectional view of the entire graft, and the magnified views of the three layers are presented in Fig. 24b. Figure 24d shows a cross-sectional view of the TPU layer and the silk/PAM interface. Figures 24e and 24f depict the inner and outer surface morphologies of the triple-layer graft.

Figure 25a presents the measured radial compliance of the triple-layer graft mentioned above. The figure depicts both the radial strength and the elasticity of the graft. In terms of radial compliance (tensile strain in radial direction), the PAM hydrogel has a value of 0.0028 MPa, electrospun TPU has a value of about 0.28 MPa, and braided silk has the highest radial compliance of about 1.0 MPa. The combination of braided silk with PAM hydrogel in a bi-layer structure has a radial strength of about 0.01 MPa, which increases to about 0.05 MPa when silk/PAM is combined with TPU to form a triple-layer structure, as illustrated in Fig. 25. The stress–strain curves describe the elastic–plastic behaviour of the mono-, bi-, and triple-layer materials. The PAM hydrogel (Fig. 25b) has identical loading and unloading curves, which reflect its near-perfect elastic behaviour. However, the difference in loading and unloading curves of braided silk (Fig. 25c) and TPU (Fig. 25d) can be observed, when tested to identical strain limits and have shown lower elastic recoveries when compared to PAM hydrogel (Fig. 25b). Therefore, the stress–strain curves qualitatively reflect the medium level of plasticity of TPU and the higher level of plasticity of the silk layer. Quantitative analyses of the level of elasticity or plasticity based on stress–strain curves can be found in Refs. [163, 164]. In addition to plasticity, the abnormality in the stress–strain curves of braided silk (Fig. 25c), which has the highest radial stress (about 1 MPa) among the materials, suggests that the silk threads are broken. Figure 25e indicates that the elastic recovery of silk improved when it was combined with PAM, and the silk became almost perfectly elastic in the triple-layer structure, as illustrated in Fig. 25f.

Composite/hybrid structures

Definitions of what constitutes a hybrid structure remain unstandardized. Various aspects of fabrication can be combined to form a 'hybrid' or 'composite' of different types of materials, different types of structures—including reinforcements, and different manufacturing methods—with the aim of attaining an artery-like performance of artificial vascular grafts. Figure 26 illustrates a graft prepared by means of automated dip-spinning and solution blow-spinning to form a hybrid structure that varies along the inner-to-outer direction in terms of fibre alignment and the number of layers. The middle layer comprises four sublayers of PCL/methacryloyl gelatin–alginate (PCL/GEAL) with a fibre orientation of ± 21°, whereas the outer layer is composed of five sublayers with a fibre orientation of ± 67°. The structure is photo-cured under UV light to enhance crosslinking in the fibrous network. Such a hybrid structure is expected to respond to

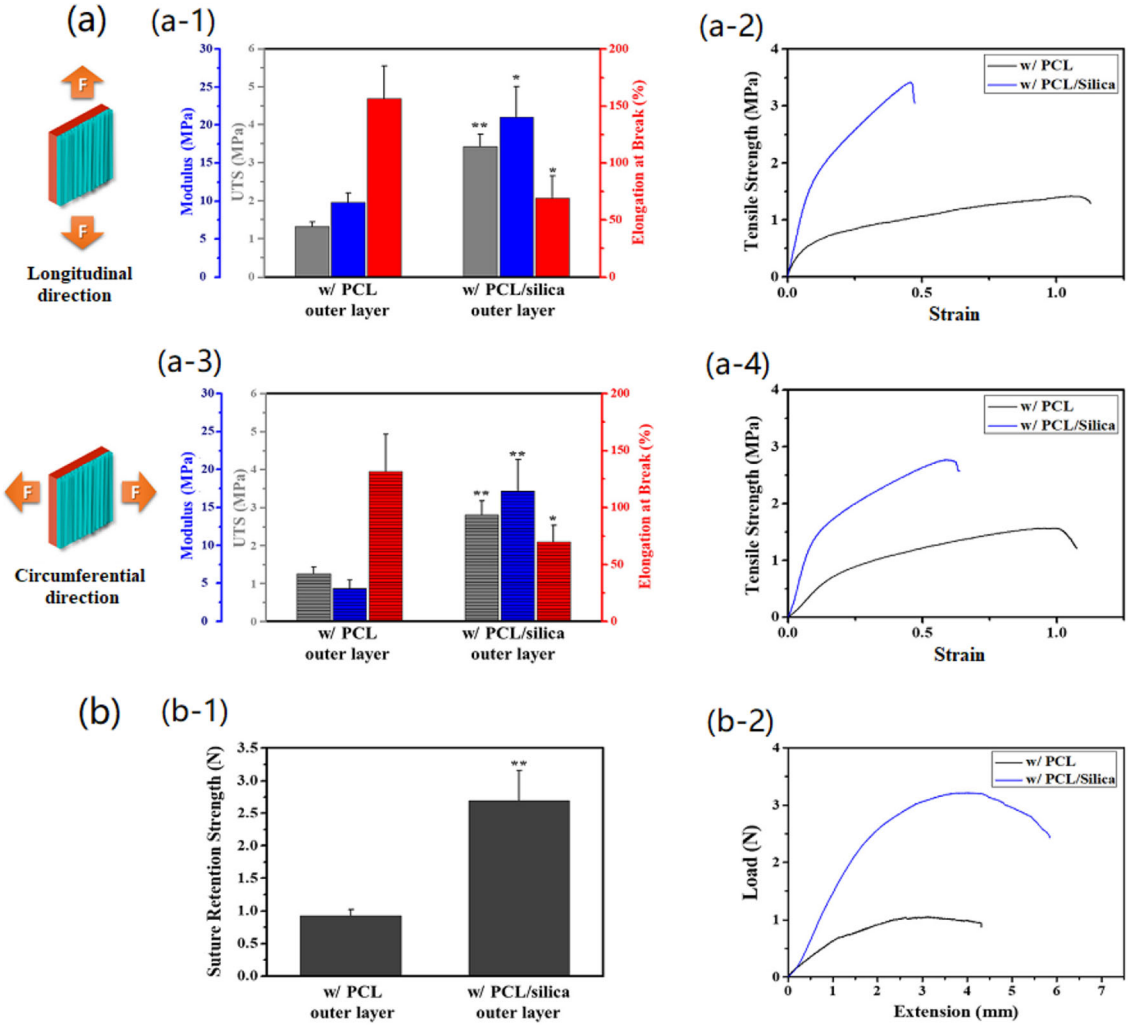

Fig. 23 **a** The ultimate tensile strength, Young's modulus and elongation of a PCL/collagen and PCL/silica bilayer graft in the axial and radial direction, and **b** suture retention in the axial direction. Reproduced from [160], Copyright 2019, CC BY Elsevier Ltd

increased blood pressure and flow rates by activating the function of each layer sequentially.

Figure 27 depicts the results of the mechanical testing of the graft described above [165]. The results indicate impressive flexibility with respect to the customization of hybrid grafts. Figure 27a indicates that the graft was manufactured with various numbers of sublayers in the central and outer layers. The tensile strengths of the five-layered matrix and four-layered biomimetic surface are close to those of the human benchmark. This allows one to derive guidelines for further refining the structural design of hybrid grafts. Figures 27b and 27c depict the axial and radial compliance of the outer layer only, which is composed of five sublayers. The axial compliance is extremely close of that of a human artery, whereas the radial compliance although not perfectly biomimetic, is still close to that of an artery. Similarly, Figs. 27d and 27e show the axial and radial compliance of the central layer, which is composed of four sublayers. This study represents significant progress in minimizing the gap between the mechanical properties of natural arteries and those of artificial vascular grafts. More details on hybrid grafts can be found in the Refs. [166–172].

The behaviour of composite grafts is affected by structural design. As shown in Fig. 27, a higher number of sublayers generally creates a stiffer graft. Fibre angles play a critical role in the mechanistic behaviour of vascular grafts. Larger fibre angles of ± 67° produce stiffer grafts with a strain of 5%–10% corresponding to 0.2 MPa of stress while smaller fibre angles of ± 21° produce ductile grafts with a strain of 30%–40%, corresponding to 0.04–0.12 MPa of stress. Optimized composite vascular grafts (i.e. five sublayers and ± 67° angles) exhibit artery-like behaviour with a strain of 0.13, corresponding to 0.14 MPa of stress. Further, composite grafts with optimized design parameters exhibit a suture retention strength of (1.40 ± 0.13) N, similar to that of the human internal thoracic artery (mammary arteries),

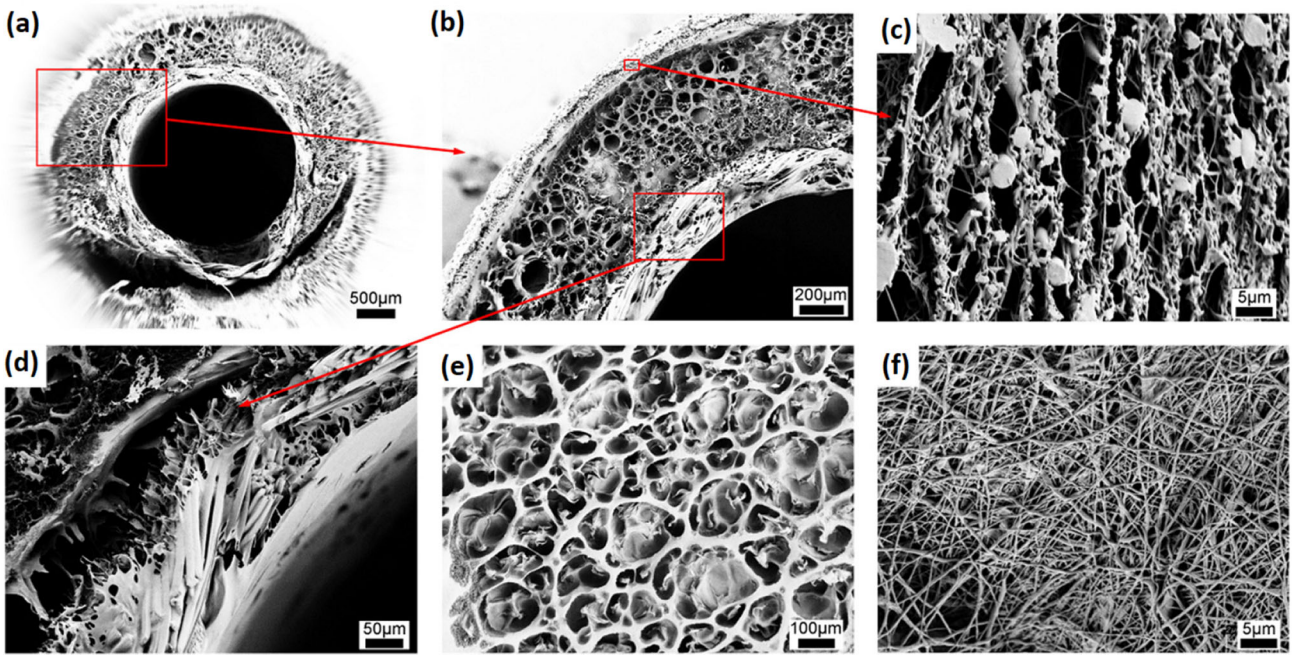

Fig. 24 **a**–**d** Cross-sectional views and **e** the inner surface and **f** the outer surface of a triple-layer silk (inner layer)/polyacrylamide (middle layer)/TPU (outer layer) graft. Reproduced from [112], Copyright 2018, with permission from Elsevier Ltd

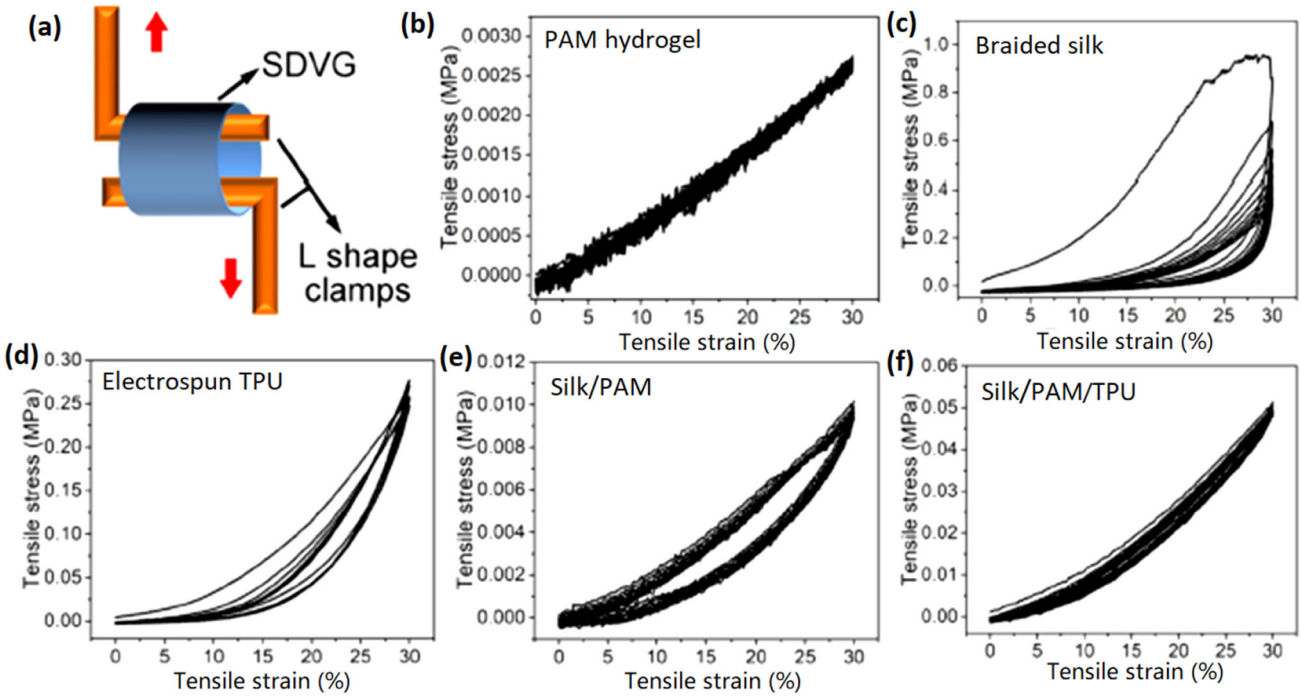

Fig. 25 **a** Radial compliance measurement setup and elastic–plastic analysis of **b** polyacrylamide (PAM) hydrogel, **c** braided silk, **d** TPU, **e** silk/PAM, and **f** silk/PAM/TPU in mono, bi-layer, and triple-layer structures. Reproduced from [112], Copyright 2018, with permission from Elsevier Ltd

i.e. (1.35 ± 0.49) N [173]. Thus, the optimised, composite vascular grafts surpass other types of grafts in mechanistic performance. The knitted grafts in [174] exhibited a high strain exceeding 0.3 under a stress of 0.2 MPa. The high elasticity caused non-compliance problems related to burst strength and artery-to-graft impedance at the suture location. Figure 28 presents an example of a composite vascular graft made from reinforced textiles [175]. The graft structure consists of rayon, spandex, nylon, and polyester, achieving human-aorta-like stress–strain behaviour in both the axial (wale) and radial (course) directions. The reinforcement of textiles and optimised material structures can help control the elasticity and stiffness of artificial vascular grafts.

Reference [176] suggests that small vascular grafts (< 5 mm in diameter) are generally used as bypass sections in intrathoracic, radial, and gastroepiploic arteries, especially for the coronary artery disease and lower-extremity arterial disease (below knee). Mid-sized grafts (5–10 mm in diameter) are usually used for replacement and bypass applications in the lower-extremity arterial disease (above knee), carotid artery, and arteriovenous fistula problems. Large vascular grafts (18–30 mm in diameter) are used as replacements in treating aortic aneurysm and aortic dissection. Degradable synthetic grafts and tissue-engineered vascular grafts made of materials such as PCL, polyglycolide (PGA), PLLA and poly(glycerol-co-sebacate) can promote self-repair, self-generation, and the growth of body tissues. PGA exhibits a high degradation rate (6–8 weeks) [54]. Nondegradable grafts have led to clinical problems such as localized argyria [177]. Therefore, various amounts of nondegradable polymers have been applied to vascular grafts to control their degradation time. One study indicates that composite grafts made of nonwoven PGA, reinforced with poly(glycolide/caprolactone) and coated with poly(lactide/caprolactone) had a six-month degradation time in an in vivo environment with grown layers of muscle cells and endothelial cells [178]. Composite vascular grafts are suitable for large-diameter blood vessels and interposition applications. When used for small-diameter blood vessels (e.g. veins), composite grafts may have safety risks related to long-term patency. Potential problems include delamination between low-dimensional features due to impact fatigue. This is because the blood pressure is 10 times [41] lower in veins than in arteries. Even simple bi-layer and tri-layer grafts can malfunction upon interlayer delamination, leading to severe abnormalities in hemodynamics.

One clinical trial indicates that a composite vascular graft made of polyester and silicon combined with diffused CD^{34+} cells and a layered structure increased the coverage of endothelial-like cells from 26 to 92% in a dog's descending thoracic aorta [179]. This advanced composite graft not only improved biological performance, but also promoted

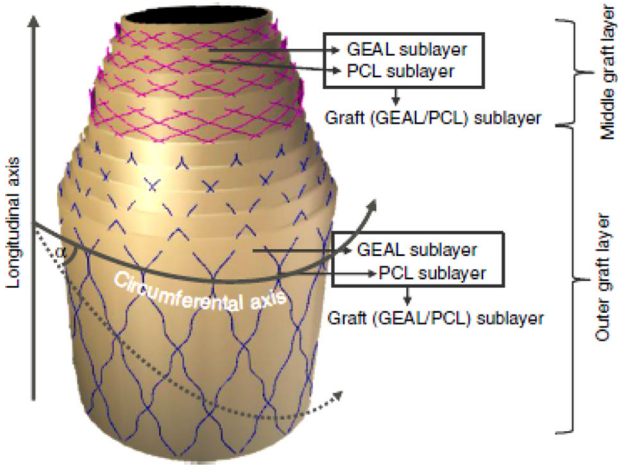

Fig. 26 A graft made of a hybrid structure of alternate layers of methacryloyl gelatin–alginate and poly(ε-caprolactone) fibres. The number of sub-layers and fibres orientation changes from the inner to the outward direction by angle, e.g. ± 21° and ± 67°. Reproduced from [165], Copyright 2019, CC BY Springer Nature

microvessel formation, a desirable feature in bone marrow applications. Although studies have investigated aspects related to material formulation [180], manufacturing [181], architecture design [182], surface functionalization [183], and accelerated hemocompatibility responses [184] of vascular grafts, rigorous preclinical and clinical trials of advanced composite vascular grafts made with complex combinations of materials, structural designs, surface engineering, and low-dimensional features remain highly needed, as to provide guidelines for their utility and practical applications [179–184].

Design criteria for mechanical functioning of vascular grafts

Surface design and matrix design play essential roles in the development of grafts with mechanical and biological properties that are similar to those of the host blood vessels. Grafts are specialized products that are produced with patient-customized specifications that vary by age, sex, physique, and location of application—such as the arm, chest, or leg. However, commercially available grafts are produced with general specifications, irrespective of patient-specific requirements. Conceivably, for the same person, textile-based grafts may function better in the chest because they provide more elasticity, whereas electrospun grafts may function better in the leg because they provide more stiffness. Similarly, the required mechanical properties of vascular grafts differ between children and adults and between men and women.

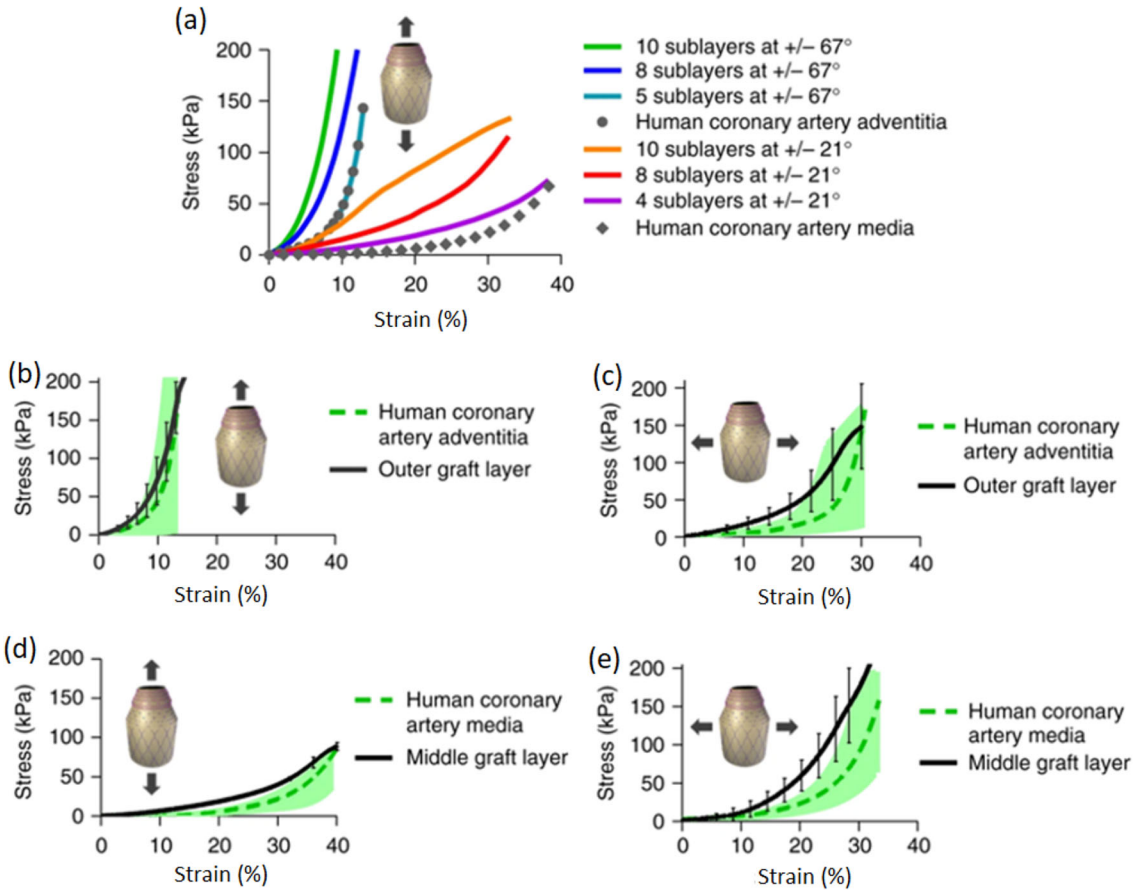

Fig. 27 **a** Optimisation of the number of methacryloyl gelatin-alginate and poly(ε-caprolactone) sub-layers in the middle and outer layer of a hybrid graft, **b** axial and **c** radial compliance of the out-layer and **d** axial and **e** radial compliance of the middle layer of the graft. Reproduced from [165], Copyright 2019, CC BY Springer Nature

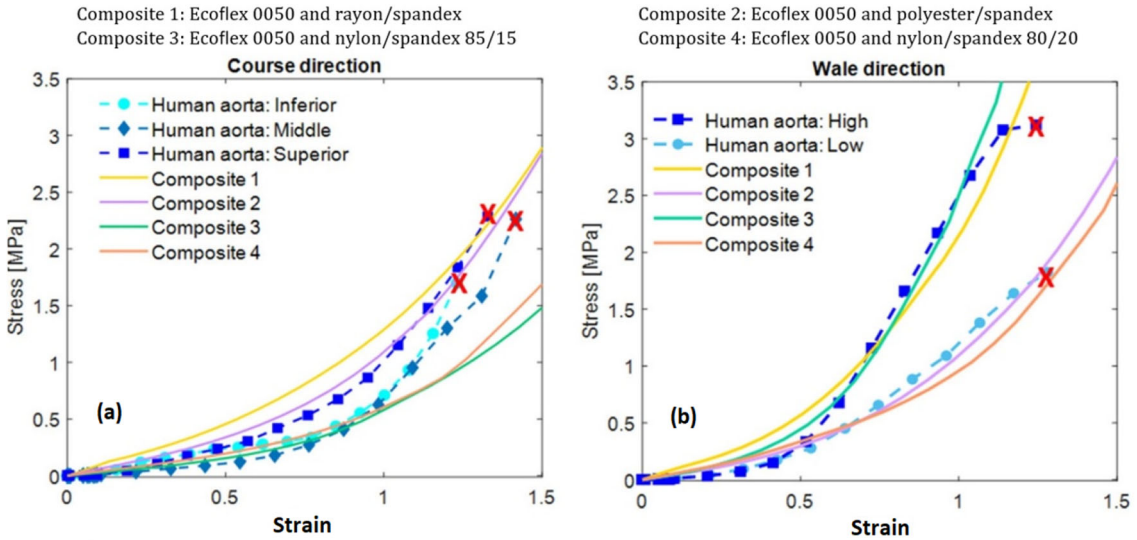

Fig. 28 Stress–strain behaviour of a textile-reinforced artificial vascular graft in comparison with a human aorta in the **a** radial (course) and **b** axial (wale) directions. Reproduced from [175], Copyright 2019, with permissions from American Chemical Society

Table 3 Key mechanical parameters of composite vascular grafts

No.	Parameter	No.	Parameter
1	Radial compliance	6	Elastic recovery
2	Longitudinal (axial) compliance	7	Tensile strength
3	Burst strength	8	Fatigue strength
4	Shear strength	9	Stiffness
5	Biomimetic surface-matrix adhesion strength	10	Buckling/rigidity

Further, no sole manufacturing method or structural design is suitable for all types of grafts due to the diversity between applications and between patients. For example, small-diameter grafts are gaining favour for use in tissue engineering methods, whereas large-diameter aortic grafts composed of textile-based materials are being researched because scaffold-based grafts may not provide the same levels of elasticity and compliance as do textile-based structures. Therefore, no general rule of thumb can be formulated for graft manufacturing. Depending on the body part in which the graft is to be applied, a combinational approach should be adopted with appropriate material selection, structural design, and manufacturing technology to deliver an appropriate level of compliance based on the mechanical parameters listed in Table 3. The unique hierarchical structural design of composite vascular grafts differentiates them from typical small- or large-diameter vascular grafts. The structural mechanics suggest that the fracture energy dissipates at interfaces [185] and mitigates crack propagation. Composite vascular grafts with numerous interfaces, including those of multiple layers, those of fibres, and those of embedded stents, exhibit high fracture toughness [185]. In the future, numerous clinical trials are necessary to provide referable guidelines on usability and demonstrate their mechanical and biomedical performance when small- and large-diameter composite vascular grafts are used. Weaving technology has been used to create novel triple-layer [102], multi-weave [138], and 3D [186] structural designs. Recent developments, such as those of tube-type fabrics [187], fabrics with a negative Poisson's ratio [188], and fabrics with structure-phase transition capabilities [189], have demonstrated promising levels of mechanical performance relative to their specified purpose. Further testing of these innovative materials with unique combinations of mechanical properties is recommended for graft manufacturing and application.

Artificial intelligence (AI) and big data are transforming present-day manufacturing norms. The role of AI in predicting graft patency was formulated in 2006 [190], and in recent years, AI has been extensively used for this purpose. AI has been demonstrated to predict ventricular function [191]—that is heart function to maintain blood supply to arteries, and detect aneurysms [192], which leads to the weakening and rupture of blood vessels. Similarly, machine-learning models based on big data are now being used to perform the screening of stenoses in grafts [193, 194] to predict abnormal contractions in blood passages. Similarly, stenoses assessments of arteriovenous grafts by neural networks have been recently reported—assessments with 86% accuracy [195]. Moreover, fuzzy-logic-based AI methods are being developed to create advanced vascular grafts by using 3D-printing methods [196]. Advancements in structural designs, the exploration of new materials, upgraded manufacturing methods, and AI applications are expected to lead to the efficient and economical production of advanced, patient-specific vascular grafts.

Conclusions

The development of new structural designs, hybrid materials engineering, and advanced manufacturing techniques in the pursuit of obtaining grafts with natural-artery-like properties is an active research area in the graft industry. This study reviews the state of the art with respect to usability, properties, and design concepts of vascular grafts. Surface design and matrix structural design of vascular grafts were also analysed, in which surface design plays an essential role in the biomimetic and mechanical functioning of grafts. The appropriate selection of natural or synthetic endothelial materials, with respect to their mechanical properties, and a safe and stable interface design is necessary to realize properly functioning vascular grafts. Similarly, computational studies aid our understanding and visualization of the efficacy of structural designs based on stress–strain and pressure distributions and can be used to derive guidelines for the development of structural designs with efficiencies that approach those of natural arteries. Vascular graft structures can be manufactured by means of tissue-engineering-based, textile-based, or architecture-based methods, and the types of structures include layered, embedded, and hybrid structures. The corresponding subcategories, such as scaffold-based, non-scaffold-based, woven, knitted, layered, embedded, and hybrid designs, are also discussed with representative examples. Different combinations of materials, structures, and manufacturing methods will regulate mechanical properties of composite vascular grafts in terms of elongation, burst strength, and tailored stiffness to offer controlled compliance and elastic recovery for achieving patient-specific requirements. Novel structural designs must be formulated and evaluated through integrated mechanical and biocompatibility analyses and clinical trials to guide practical applications of vascular grafts for end-users in surgery.

Acknowledgements The authors would like to thank the Innovation and Technology Fund-The Hong Kong Research Institute of Textiles and Apparel (ITF-HKRITA, PRP/059/19TI), and the Department General Research Fund, the Hong Kong Polytechnic University (G-UAHB) for supporting this study.

Author contributions RL and AWZ planned the manuscript. AWZ contributed to writing—original draft. RL contributed to writing—review and editing, funding acquisition. XBW contributed to discussion and review.

Declarations

Conflict of interest The authors declare that they have no conflict of interest.

Ethical approval This study does not contain any studies with human or animal subjects performed by any of the authors.

References

1. Yawn R, Hunter JB, Sweeney AD et al (2015) Cochlear implantation: a biomechanical prosthesis for hearing loss. F1000Prime Rep 7:45
2. Amanzadeh K, Elham R, Jafarzadeur E (2017) Effects of single-segment Intacs implantation on visual acuity and corneal topographic indices of keratoconus. J Curr Ophthalmol 29:189–193. https://doi.org/10.1016/j.joco.2016.10.004
3. Rabinowitz YS (2006) INTACS for keratoconus. Int Ophthalmol Clin 46:91–103. https://doi.org/10.1097/00004397-200604630-00009
4. Nordquist WD, Krutchkoff DJ (2014) The custom endosteal implant: histology and case report of a retrieved maxillary custom osseous-integrated implant nine years in service. J Oral Implantol 40:195–201. https://doi.org/10.1563/aaid-joi-d-11-00218
5. Beddis H, Lello S, Cunliffe J et al (2012) Subperiosteal implants. Br Dent J 212:4. https://doi.org/10.1038/sj.bdj.2012.6
6. Grecchi F, Bianchi AE, Siervo S et al (2017) A new surgical and technical approach in zygomatic implantology. Oral Implantol (Rome) 10:197–208
7. Koszuta P, Grafka A, Koszuta A et al (2015) Effects of selected factors on the osseointegration of dental implants. Prz Menopauzalny 14:184–187. https://doi.org/10.5114/pm.2015.54343
8. Cuenin MF, Billman MA, Kudryk L et al (1997) Estrogenic hormones and dental implant therapy: the effects of estrogen and progesterone levels on osseointegration of dental implants. Mil Med 162:582. https://doi.org/10.1093/milmed/162.9.582
9. Guo J, Reside G, Cooper LF (2011) Full-mouth rehabilitation of a patient with gastroesophageal reflux disease: a clinical report. J Prosthodont 2:S9-13. https://doi.org/10.1111/j.1532-849x.2011.00785.x
10. Altay MA, Sindel A, Özalp Ö et al (2019) Proton pump inhibitor intake negatively affects the osseointegration of dental implants: a retrospective study. J Korean Assoc Oral Maxillofac Surg 45:135–140. https://doi.org/10.5125/jkaoms.2019.45.3.135
11. Aghaloo T, Pi-Anfruns J, Moshaverinia A et al (2019) The effects of systemic diseases and medications on osseointegration: a systematic review. Int J Oral Maxillofac Implant Suppl 34:s35–s49
12. Salzmann SN, Plais N, Shue J et al (2017) Lumbar disc replacement surgery-successes and obstacles to widespread adoption. Curr Rev Musculoskelet Med 10:153–159. https://doi.org/10.1007/s12178-017-9397-4
13. Heckmann N, Tezuka T, Bonder RJ et al (2021) Functional anatomy of the hip joint. J Arthroplasty 36:374–378. https://doi.org/10.1016/j.arth.2020.07.065
14. Vaienti E, Scita G, Ceccarelli F et al (2017) Understanding the human knee and its relationship to total knee replacement. Acta Biomed 88(2S):6–16
15. Vasukutty NL, Middleton RG, Young P et al (2014) A double mobility acetabular implant for primary hip arthroplasty in patients at high risk of dislocation. Ann R Coll Surg Engl 96(8):597–601. https://doi.org/10.1308/003588414x14055925058391
16. Slovut DP, Lipsitz EC (2012) Surgical technique and peripheral artery disease. Circulation 126:1127–1138. https://doi.org/10.1161/circulationaha.111.059048
17. Lazar HL, Menzoian JO (1998) Coronary artery bypass grafting in patients with cerebrovascular disease. Ann Thoracic Surg 66:968–974. https://doi.org/10.1016/s0003-4975(98)00687-0
18. Walter J, Magometschnigg H (2007) The role of vein grafts in peripheral vascular disease and carotid artery disease. Eur Surg 39:76–82. https://doi.org/10.1007/s10353-007-0317-5
19. Wawrzyńska M, Bil-Lula I, Krzywonos-Zawadzka A et al (2018) Biocompatible carbon-based coating as potential endovascular material for stent surface. BioMed Res Int. https://doi.org/10.1155/2018/2758347
20. Ricco JB, Assadian O (2011) Antimicrobial silver grafts for prevention and treatment of vascular graft infection. Semin Vasc Surg 24:234–241. https://doi.org/10.1053/j.semvascsurg.2011.10.006
21. Schild AF, Baltodano NM, Alfieri K et al (2004) New graft for low friction tunneling in vascular access surgery. J Vasc Access 5(1):19–24. https://doi.org/10.1177/112972980400500105
22. Narayanan SNS, Park IS, Lee MH (2014) Strategies to improve the corrosion resistance of microarc oxidation (MAO) coated magnesium alloys for degradable implants: prospects and challenges. Prog Mater Sci 60:1–71. https://doi.org/10.1016/j.pmatsci.2013.08.002
23. Wong LY, Liew AST, Weng WT et al (2018) Projecting the burden of chronic kidney disease in a developed country and its implications on public health. Int J Nephrol 2018:5196285. https://doi.org/10.1155/2018/5196285
24. Global vascular graft market size, share, trends, COVID-19 impact and growth analysis report - segmented by raw material, product, end-user and region – industry forecast (2022 to 2027), 2022. ID 7419, Market Data Forecast, India. https://www.marketdataforecast.com/market-reports/vascular-graft-treatment-market. Accessed 29 March 2022
25. Vascular Graft Market - Global opportunity analysis and industry forecast, 2017–2023. Report ID: 5139456. Report Buyer Ltd. United Kingdom 2017. https://www.reportbuyer.com/product/5139456/vascular-graft-market-global-opportunity-analysis-and-industry-forecast.html Accessed 14 March 2022

26. Vascular graft market - growth, trends, covid-19 impact, and forecasts (2022 - 2027). Mordor Intelligence. https://www.mordorintelligence.com/industry-reports/vascular-graft-market. Accessed 30 March 2021
27. Ugalmugle S (2021) Vascular graft market size by raw material (polyester grafts, expanded polytetrafluoroethylene grafts, polyurethane grafts, biosynthetic grafts), by application (Endovascular aneurysm repair, {abdominal aortic aneurysm repair, thoracic aortic aneurysm repair}, reripheral vascular repair, hemodialysis access), by end-use (hospitals, ambulatory surgical centers), industry analysis report, regional outlook, application potential, competitive market share & forecast, 2018 – 2024. Report ID DM12492, Global Market Insights Inc. USA 2018. Accessed: 30/03/2021 https://www.gminsights.com/industry-analysis/vascular-graft-market. Accessed 30 March 2021
28. Lemson MS, Tordoir JHM, Daemen MJAP, Kitslaar PJEHM (2000) Intimal hyperplasia in vascular grafts. Eur J Vascul Endovascul Surg 19:336–350. https://doi.org/10.1053/ejvs.1999.1040
29. Hibino N, McGillicuddy E, Matsumura G et al (2010) Late-term results of tissue-engineered vascular grafts in humans. J Thorac Cardiovasc Surg 139:431–436. https://doi.org/10.1016/j.jtcvs.2009.09.057
30. Neufurth M, Wang X, Tolba E et al (2015) Modular small diameter vascular grafts with bioactive functionalities. PLoS ONE 10:e0133632. https://doi.org/10.1371/journal.pone.0133632
31. Popryadukhin PV, Popov GI, Yukina GY et al (2017) Tissue-engineered vascular graft of small diameter based on electrospun polylactide microfibers. Int J Biomater 9034186:1–10. https://doi.org/10.1155/2017/9034186
32. Etz CD, Homann T, Silovitz D et al (2007) Vascular graft replacement of the ascending and descending aorta: do Dacron grafts grow? Ann Thorac Surg 84:1206–1213. https://doi.org/10.1016/j.athoracsur.2007.05.034
33. Hanson SR, Harker LA (1987) Vascular graft thrombus formation. Ann N Y Acad Sci 516:653–661. https://doi.org/10.1111/j.1749-6632.1987.tb33082.x
34. Karayannacos PE, Rittgers SE, Kakos GS et al. (1980) Potential role of velocity and wall tension in vein graft failure. J Cardiovasc Surg (Torino) 21:171–178. https://pubmed.ncbi.nlm.nih.gov/7364860/
35. Sarkar S, Salacinski HJ, Hamilton G et al (2006) The mechanical properties of infrainguinal vascular bypass grafts: their role in influencing patency. Eur J Vascul Endovascul Surg 31:627–636. https://doi.org/10.1016/j.ejvs.2006.01.006
36. Singh C, Wang X, Morsi Y et al (2017) Importance of stent-graft design for aortic arch aneurysm repair. AIMS Bioeng 4(1):133–150. https://doi.org/10.3934/bioeng.2017.1.133
37. Radke D, Jia W, Sharma D et al (2018) Tissue engineering at the blood-contacting surface: a review of challenges and strategies in vascular graft development. Adv Healthc Mater 7:e1701461. https://doi.org/10.1002/adhm.201701461
38. Salacinski HJ, Goldner S, Giudiceandrea A et al (2001) The mechanical behavior of vascular grafts: a review. J Biomater Appl 15:241–278. https://doi.org/10.1106/NA5T-J57A-JTDD-FD04
39. Cecchi E, Giglioli C, Valente S et al (2011) Role of hemodynamic shear stress in cardiovascular disease. Atherosclerosis 214:249–256. https://doi.org/10.1016/j.atherosclerosis.2010.09.008
40. Rana A, Westein E, Niego B et al (2019) Shear-dependent platelet aggregation: mechanisms and therapeutic opportunities. Front Cardiovasc Med 6:141. https://doi.org/10.3389/fcvm.2019.00141
41. Camasão DB, Mantovani D (2021) The mechanical characterization of blood vessels and their substitutes in the continuous quest for physiological-relevant performances. A Crit Rev Mater Today Bio 10:100106. https://doi.org/10.1016/j.mtbio.2021.100106
42. Ozturk N, Sucu N, Comelekoglu U et al (2013) Pressure applied during surgery alters the biomechanical properties of human saphenous vein graft. Heart Vessels 28:237–245. https://doi.org/10.1007/s00380-012-0245-6
43. Danpinid A, Luo J, Vappou J, Terdtoon P, Konofagou EE (2010) In vivo characterization of the aortic wall stress-strain relationship. Ultrasonics 50(7):654–665. https://doi.org/10.1016/j.ultras.2010.01.003
44. Zhao S, Gu L, Froemming SR (2012) Effects of arterial strain and stress in the prediction of restenosis risk: computer modeling of stent trials. Biomed Eng Lett 2:158–163. https://doi.org/10.1007/s13534-012-0067-6
45. Marasco A (2021) Vascular grafts. Presentation. Mcmaster University, Canada. https://www.ece.mcmaster.ca/~ibruce/courses/EE3BA3_2011/EE3BA3notes/EE3BA3_presentation01.pdf. Accesses 01 January 2021
46. Daye D, Walker TG (2018) Complications of endovascular aneurysm repair of the thoracic and abdominal aorta: evaluation and management. Cardiovasc Diagn Ther 8:S138–S156
47. Shakarchi J, Nath J, McGrogan D et al (2015) End-stage vascular access failure: can we define and can we classify? Clin. Kidney J 8:590–593. https://doi.org/10.1093/ckj/sfv055
48. Wain RA, Marin ML, Ojki T et al (1998) Endoleaks after endovascular graft treatment of aortic aneurysms: classification, risk factors, and outcome. J Vasc Surg 27:69–80. https://doi.org/10.1016/s0741-5214(98)70293-9
49. Exton RJ, Galland RB (2007) Major groin complications following the use of synthetic grafts. Eur J Vasc Endovasc Surg 34:188–190. https://doi.org/10.1016/j.ejvs.2007.03.012
50. Thevendran G, Lord R, Sarraf KM (2009) Serous leak, a rare complication of polytetrafluoroethylene grafts: a case report. Cases J 2:195. https://doi.org/10.1186/1757-1626-2-195
51. Wilson WR, Bower TC, Creager MA et al (2016) Vascular graft infections, mycotic aneurysms, and endovascular infections: a scientific statement from the American heart association. Circulation 134:e412–e460. https://doi.org/10.1161/cir.0000000000000457
52. Turtiainen J, Hakala T (2014) Surgical wound infections after peripheral vascular surgery. Scand J Surg 103:226–231. https://doi.org/10.1177/1457496913514384
53. Vascular prosthesis for coronary artery bypass. Biotextiles 2014. https://biotextiles2014.wordpress.com/vascular-prosthesis-for-coronary-artery-bypass.Accessed 1 January 2022
54. Durán-Rey D, Crisóstomo V, Sánchez-Margallo JA et al (2021) Systematic review of tissue-engineered vascular grafts. Front Bioeng Biotechnol 9:771400. https://doi.org/10.3389/fbioe.2021.771400
55. Ricco JB, Assadian O (2011) Antimicrobial silver grafts for prevention and treatment of vascular graft infection. Semin Vasc Surg 24(4):234–241. https://doi.org/10.1053/j.semvascsurg.2011.10.006
56. Jeanmonod P, Laschke MW, Gola N et al (2013) Silver acetate coating promotes early vascularization of Dacron vascular grafts without inducing host tissue inflammation. J Vasc Surg 58(6):1637–1643. https://doi.org/10.1016/j.jvs.2013.02.012
57. Wulff B, Stahlhoff S, Vonthein R et al (2017) Biomimetic heparan sulfate-like coated ePTFE grafts reduce in-graft neointimal hyperplasia in ovine carotids. Ann Vasc Surg 40:274–284. https://doi.org/10.1016/j.avsg.2016.09.015
58. Moore WS (2012) Vascular and endovascular surgery E-book: a comprehensive review. United Kingdom: Elsevier Health Sciences. Hardcover ISBN: 9780323480116, eBook ISBN: 9780323527712

59. Thomson LA, Law FC, Rushton N et al (1991) Biocompatibility of diamond-like carbon coating. Biomaterials 12(1):37–40. https://doi.org/10.1016/0142-9612(91)90129-x
60. Orrit-Prat J, Bonet R, Rupérez E et al (2021) Bactericidal silver-doped DLC coatings obtained by pulsed filtered cathodic arc co-deposition. Surf Coat Tech 15(411):126977. https://doi.org/10.1016/j.surfcoat.2021.126977
61. Roy ME, Whiteside LA, Xu J et al (2010) Diamond-like carbon coatings enhance the hardness and resilience of bearing surfaces for use in joint arthroplasty. Acta Biomater 6(4):1619–1924. https://doi.org/10.1016/j.actbio.2009.10.037
62. Field SK, Jarratt M, Teer DG (2004) Tribological properties of graphite-like and diamond-like carbon coatings. Tribol Int 37(11–12):949–956. https://doi.org/10.1016/j.triboint.2004.07.012
63. Fujii Y, Goyama T, Muraoka G et al (2019) Effects of diamond-like-carbon coating for ePTFE artificial vascular graft as arteriovenous graft. Eur J Vasc Endovasc Surg 58(6):e419–e420. https://doi.org/10.1016/j.ejvs.2019.06.1065
64. Cardiovascular implants and extracorporeal systems — vascular prostheses — tubular vascular grafts and vascular patches. ISO 7198 2016
65. Komutrattananont P, Mahakkanukrauh P, Das S (2019) Morphology of the human aorta and age-related changes: anatomical facts. Anat Cell Biol 52(2):109–114. https://doi.org/10.5115/acb.2019.52.2.109
66. Jorgensen CS, Paaske WP (1998) Physical and mechanical properties of ePTFE stretch vascular grafts determined by time-resolved scanning acoustic microscopy. Eur J Vasc Endovasc Surg 15:416–422. https://doi.org/10.1016/S1078-5884(98)80203-7
67. Chiu LLY, Radisic M (2010) Scaffolds with covalently immobilized VEGF and Angiopoietin-1 for vascularization of engineered tissues. Biomaterials 31:226–241. https://doi.org/10.1016/j.biomaterials.2009.09.039
68. Ricard-Blum S (2011) The collagen family. Cold Spring Harb Perspect Bio 3:a004978. https://doi.org/10.1101/cshperspect.a004978
69. Berard X, Stecken L, Pinaquy JB et al (2016) Comparison of the antimicrobial properties of silver impregnated vascular grafts with and without triclosan. Eur J Vasc Endovasc Surg 51(2):285–292. https://doi.org/10.1016/j.ejvs.2015.10.016
70. Khan OF, Sefton MV (2011) Endothelialized biomaterials for tissue engineering applications in vivo. Trends Biotech 29:379–387. https://doi.org/10.1016/j.tibtech.2011.03.004
71. Wu HC, Wang TW, Kang PL et al (2007) Coculture of endothelial and smooth muscle cells on a collagen membrane in the development of a small-diameter vascular graft. Biomaterials 28:1385–1392. https://doi.org/10.1016/j.biomaterials.2006.11.012
72. Leung BM, Sefton MV (2007) A modular tissue engineering construct containing smooth muscle cells and endothelial cells. Ann Biomed Eng 35:2039–2049. https://doi.org/10.1007/s10439-007-9380-0
73. Toole BP, Wight TN, Tammi MI (2002) Hyaluronan–cell interactions in cancer and vascular disease. J Biol Chem 277:4593–4596. https://doi.org/10.1074/jbc.r100039200
74. Chen WYJ, Abatangelo G (1999) Functions of hyaluronan in wound repair. Wound Repair Regen 7:79–89. https://doi.org/10.1046/j.1524-475x.1999.00079.x
75. Zavan B, Vindigni V, Lepidi S et al (2008) Neoarteries grown in vivo using a tissue engineered hyaluronan-based scaffold. FASEB J 22:2853–2861. https://doi.org/10.1096/fj.08-107284
76. Tang ZCW, Liao WY, Tang AC et al (2011) The enhancement of endothelial cell therapy for angiogenesis in hindlimb ischemia using hyaluronan. Biomaterials 32:75–86. https://doi.org/10.1016/j.biomaterials.2010.08.085
77. Draget KI, Taylor C (2011) Chemical, physical and biological properties of alginates and their biomedical implications. Food Hydrocolloids 25:251–256. https://doi.org/10.1016/j.foodhyd.2009.10.007
78. Silva EA, Kim ES, Kong HJ et al (2008) Material-based deployment enhances efficacy of endothelial progenitor cells. Proc Natl Acad Sci USA 105:14347–14352. https://doi.org/10.1073/pnas.0803873105
79. Yu J, Gu Y, Du KT et al (2009) The effect of injected RGD modified alginate on angiogenesis and left ventricular function in a chronic rat infarct model. Biomaterials 30:751–756. https://doi.org/10.1016/j.biomaterials.2008.09.059
80. Laschke MW, Rücker M, Jensen G et al (2008) Incorporation of growth factor containing Matrigel promotes vascularization of porous PLGA scaffolds. J Biomed Mater Res A 85:397–407. https://doi.org/10.1002/jbm.a.31503
81. Shaikh FM et al (2008) Fibrin: a natural biodegradable scaffold in vascular tissue engineering. Cells Tissues Organs 188:333–346. https://doi.org/10.1159/000139772
82. Chen X, Aledia AS, Ghajar CM et al (2009) Prevascularization of a fibrin-based tissue construct accelerates the formation of functional anastomosis with host vasculature. Tissue Eng Part A 15:1363–1371. https://doi.org/10.1089/ten.tea.2008.0314
83. Unger RE, Ghanaati S, Orth C et al (2010) The rapid anastomosis between prevascularized networks on silk fibroin scaffolds generated in vitro with cocultures of human microvascular endothelial and osteoblast cells and the host vasculature. Biomaterials 31:6959–6967. https://doi.org/10.1016/j.biomaterials.2010.05.057
84. Wang X, Zhang X, Castellot J et al (2008) Controlled release from multilayer silk biomaterial coatings to modulate vascular cell responses. Biomaterials 29:894–903. https://doi.org/10.1016/j.biomaterials.2007.10.055
85. Jung JP, Nagaraj AK, Fox EK et al (2009) Co-assembling peptides as defined matrices for endothelial cells. Biomaterials 30:2400–2410. https://doi.org/10.1016/j.biomaterials.2009.01.033
86. Sieminski AL, Semino CE, Gong H et al (2008) Primary sequence of ionic self-assembling peptide gels affects endothelial cell adhesion and capillary morphogenesis. J Biomed Mater Res A 87:494–504. https://doi.org/10.1002/jbm.a.31785
87. Hamada Y, Egusa H, Kaneda Y et al (2007) Synthetic osteopontin-derived peptide SVVYGLR can induce neovascularization in artificial bone marrow scaffold biomaterials. Dent Mater J 26:487–492. https://doi.org/10.4012/dmj.26.487
88. Ott HC, Matthiesen TS, Goh SK et al (2008) Perfusion-decellularized matrix: using nature's platform to engineer a bioartificial heart. Nat Med 14:213–221. https://doi.org/10.1038/nm1684
89. Ott HC, Clippinger B, Conrad C et al (2010) Regeneration and orthotopic transplantation of a bioartificial lung. Nat Med 16:927–933. https://doi.org/10.1038/nm.2193
90. Petersen TH, Calle EA, Zhao L et al (2010) Tissue-engineered lungs for in vivo implantation. Science 329:538–541. https://doi.org/10.1126/science.1189345
91. Zhao Y, Zhang S, Zhou J et al (2010) The development of a tissue-engineered artery using decellularized scaffold and autologous ovine mesenchymal stem cells. Biomaterials 31:296–307. https://doi.org/10.1016/j.biomaterials.2009.09.049
92. Pektok E, Nottelet B, Tille JC et al (2008) Degradation and healing characteristics of small-diameter poly(epsilon-caprolactone) vascular grafts in the rat systemic arterial circulation. Circulation 118:2563–2570. https://doi.org/10.1161/circulationaha.108.795732
93. Serrano MC, Pagani R, Vallet-Regí M et al (2009) Nitric oxide production by endothelial cells derived from blood progenitors

cultured on NaOH-treated polycaprolactone films: a biofunctionality study. Acta Biomater 5:2045–2053. https://doi.org/10.1016/j.actbio.2009.02.034
94. Santos MI, Fuchs S, Gomes ME et al (2007) Response of micro- and macrovascular endothelial cells to starch-based fiber meshes for bone tissue engineering. Biomaterials 28:240–248. https://doi.org/10.1016/j.biomaterials.2006.08.006
95. Kraehenbuehl TP, Ferreira LS, Hayward AM et al (2011) Human embryonic stem cell-derived microvascular grafts for cardiac tissue preservation after myocardial infarction. Biomaterials 32:1102–1109. https://doi.org/10.1016/j.biomaterials.2010.10.005
96. Phelps EA, Landázuri N, Thulé PM et al (2010) Bioartificial matrices for therapeutic vascularization. Proc Natl Acad Sci USA 107:3323–3328. https://doi.org/10.1073/pnas.0905447107
97. Madden LR, Mortisen DJ, Sussman EM et al (2010) Proangiogenic scaffolds as functional templates for cardiac tissue engineering. Proc Natl Acad Sci USA 107:15211–15216. https://doi.org/10.1073/pnas.1006442107
98. Ekaputra AK, Prestwich GD, Cool SM et al (2008) Combining electrospun scaffolds with electrosprayed hydrogels leads to three-dimensional cellularization of hybrid constructs. Biomacromol 9:2097–2103. https://doi.org/10.1021/bm800565u
99. Zamani M, Khafaji M, Naji M et al (2017) A biomimetic heparinized composite silk-based vascular scaffold with sustained antithrombogenicity. Sci Rep 7:4455. https://doi.org/10.1038/s41598-017-04510-1
100. Franke U, Jurmann MJ, Uthoff K et al (1997) In vivo morphology of woven, collagen-sealed Dacron prostheses in the thoracic aorta. Ann Thorac Surg 64:1096–1098. https://doi.org/10.1016/s0003-4975(97)00802-3
101. Singh C, Wong CS, Wang X (2015) Medical textiles as vascular implants and their success to mimic natural arteries. J Funct Biomater 6:500–525. https://doi.org/10.3390/jfb6030500
102. Guidoin R, Marceau D, Couture J et al (1989) Collagen coatings as biological sealants for textile arterial prostheses. Biomaterials 10:156. https://doi.org/10.1016/0142-9612(89)90018-5
103. Francesco C, Nele P, Sandra VV et al (2019) Collagen-based tissue engineering strategies for vascular medicine. Front Bioeng Biotech 7:166. https://doi.org/10.3389/fbioe.2019.00166
104. Stegmann T, Haverich A, Borst HG (1986) Clinical experience with a new collagen-coated Dacron double-velour prosthesis. Thorac Cardiovasc Surgeon 34:54–56. https://doi.org/10.1055/s-2007-1020374
105. Noishiki Y, Marat D, Yamane Y et al (1996) A collagen coated fabric vascular prosthesis as a punctureable A-V shunt. ASAIO J 42:M687-693. https://doi.org/10.1097/00002480-199609000-00075
106. Aytemiz D, Sakiyama W, Suzuki Y et al (2013) Small-diameter silk vascular grafts (3 mm diameter) with a double-raschel knitted silk tube coated with silk fibroin sponge. Adv Healthcare Mater 2:361–368. https://doi.org/10.1002/adhm.201200227
107. Xu W, Zhou F, Ouyang C et al (2010) Mechanical properties of small-diameter polyurethane vascular grafts reinforced by weft-knitted tubular fabric. J Biomed Mater Res A 92:1–8. https://doi.org/10.1002/jbm.a.32333
108. Sahoo S, Cho-Hong JG, Siew-Lok T (2007) Development of hybrid polymer scaffolds for potential applications in ligament and tendon tissue engineering. Biomed Mater 2:169–173. https://doi.org/10.1088/1748-6041/2/3/001
109. Konrad P, Dougan P, Bergqvist D (1992) Acute thrombogenicity of collagen coating of Dacron grafts: an experimental study in sheep. Eur J Vasc Surg 6:67–72. https://doi.org/10.1016/s0950-821x(05)80097-0
110. Suehiro K, Hata T, Yoshitaka H et al (2003) Impact of collagen-coated and gelatine-impregnated woven Dacron branched grafts on the early postoperative period. Japanese J Thorac Cardiovasc Surg 51:641–644. https://doi.org/10.1007/s11748-003-0001-z
111. Zhang B, Xu Y, Ma S, Wang L, Liu C et al (2021) Small-diameter polyurethane vascular graft with high strength and excellent compliance. J Mech Behav Biomed Mater 121:104614. https://doi.org/10.1016/j.jmbbm.2021.104614
112. Mi HY, Jiang Y, Jing X et al (2019) Fabrication of triple-layered vascular grafts composed of silk fibers, polyacrylamide hydrogel, and polyurethane nanofibers with biomimetic mechanical properties. Mater Sci Eng C 98:241–249. https://doi.org/10.1016/j.msec.2018.12.126
113. Kato M, Ohnishi K, Kaneko M et al. (1996) New graft-implanting method for thoracic aortic aneurysm or dissection with a stented graft. Circulation 94:II188–II193. https://pubmed.ncbi.nlm.nih.gov/8901744/
114. Suto Y, Yasuda K, Shiiya N et al (1996) Stented elephant trunk procedure for an extensive aneurysm involving distal aortic arch and descending aorta. J Thorac Cardiovasc Surg 112:1389–1390. https://doi.org/10.1016/s0022-5223(96)70157-5
115. Chavan A, Karck M, Hagl C et al (2005) Hybrid endograft for one-step treatment of multisegment disease of the thoracic aorta. J Vasc Interv Radiol 16:823–829. https://doi.org/10.1097/01.rvi.0000159205.00299.97
116. Ricco JB, Assadian A, Schneider F et al (2012) In vitro evaluation of the antimicrobial efficacy of a new silver-triclosan vs a silver collagen-coated polyester vascular graft against methicillin-resistant Staphylococcus aureus. J Vasc Surg 55:823–829. https://doi.org/10.1016/j.jvs.2011.08.015
117. Gorlitzer M, Weiss G, Thalmann M et al (2007) Combined surgical and endovascular repair of complex aortic pathologies with a new hybrid prosthesis. Ann Thorac Surg 84:1971–1976. https://doi.org/10.1016/j.athoracsur.2007.07.010
118. Fan H, Lu H, Gao LJ (2015) A Computational model for biomechanical effects of arterial compliance mismatch. Appl Bionics Biomech 213236:6. https://doi.org/10.1155/2015/213236
119. Kassab GS, Navia JA (2006) Biomechanical considerations in the design of graft: the homeostasis hypothesis. Annu Rev Biomed Eng 8:499–535. https://doi.org/10.1146/annurev.bioeng.8.010506.105023
120. Bai Z, Zhu L (2019) Simulation of blood flow past a distal arteriovenous-graft anastomosis at low Reynolds numbers. Phys Fluids 31:091902. https://doi.org/10.1063/1.5099635
121. Bathe M, Kamm RD (1999) A fluid-structure interaction finite element analysis of pulsatile blood flow through a compliant stenotic artery. J Biomech Eng 121(4):361–369. https://doi.org/10.1115/1.2798332
122. Nerem RM (1992) Vascular fluid mechanics, the arterial wall, and atherosclerosis. J Biomech Eng 114:274–282. https://doi.org/10.1115/1.2891384
123. Marshall I, Zhao S, Papathanasopoulou P et al (2004) (2004) MRI and CFD studies of pulsatile flow in healthy and stenosed carotid bifurcation models. J Biomech 37(5):679–687. https://doi.org/10.1016/j.jbiomech.2003.09.032
124. Han HC (2007) A biomechanical model of artery buckling. J Biomech 40(16):3672–3678. https://doi.org/10.1016/j.jbiomech.2007.06.018
125. Ku DN, Giddens DP, Zarins CK et al (1985) Pulsatile flow and atherosclerosis in the human carotid bifurcation: positive correlation between plaque location and low and oscillating shear stress. Arteriosclerosis 5:293–302. https://doi.org/10.1161/01.atv.5.3.293
126. Tang D, Yang C, Walker H et al (2002) Simulating cyclic artery compression using a 3D unsteady model with fluid-structure interactions. Comput Struct 80:1651–1665. https://doi.org/10.1016/S0045-7949(02)00111-6

127. Pedley TJ (1980) The fluid mechanics of large blood vessels. Cambridge University Press, Cambridge
128. Loth F, Jones SA, Zarins CK et al (2002) Relative contribution of wall shear stress and injury in experimental intimal thickening at PTFE end-to-side arterial anastomoses. J Biomech Eng 124:44–51
129. Abraham JP, Sparrow EM, Lovik RD (2008) Unsteady, three-dimensional fluid mechanic analysis of blood flow in plaque-narrowed and plaque-freed arteries. Int J Heat Mass Transf 51:5633–5641. https://doi.org/10.1016/j.ijheatmasstransfer.2008.04.038
130. Naughton NM, Plourde BD, Stark JR et al (2014) Impacts of waveforms on the fluid flow, wall shear stress, and flow distribution in cerebral aneurysms and the development of a universal reduced pressure. J Biomed Sci Eng 7:7–14. https://doi.org/10.4236/jbise.2014.71002
131. Boerboom RA, Rubbens MP, Driessen NJB et al (2008) Effect of strain magnitude on the tissue properties of engineered cardiovascular constructs. Ann Biomed Eng 36:244–253. https://doi.org/10.1007/s10439-007-9413-8
132. Lu YL, Lu XY, Zhuang LX et al. (2002) Breaking symmetry in non-planar bifurcations: distribution of flow and wall shear stress. Biorheology 39:431–436. https://pubmed.ncbi.nlm.nih.gov/12122263
133. Balossino R, Gervaso F, Migliavacca F et al (2008) Effects of different stent designs on local hemodynamics in stented arteries. J Biomech 41:1053–1061. https://doi.org/10.1016/j.jbiomech.2007.12.005
134. Woven fabric finishing equipment for groundscare. Patent No KR101756081B1 2017 South Korea. https://patents.google.com/patent/KR101756081B1/en
135. A kind of elastomeric overmold line woven fabric. Patent No CN209508518U 2019 China. https://patents.google.com/patent/CN209508518U/en
136. With the shuttle-woven fabric and its production technology for unidirectionally leading suction function. Patent No CN107083605B 2019 China. https://patents.google.com/patent/CN107083605B/en
137. Woven fabric. Patent No USD826577S1 2018 USA. https://patents.google.com/patent/USD826577S1/
138. Naik K, Sridev E (2002) An analytical method for thermoelastic analysis of 3D orthogonal interlock woven composites. J Reinf Plast Compos 21:13
139. Kumar B, Hu J (2018) Woven fabric structures and properties. In: Miao M, Xin JH (eds) Engineering of high-performance textiles. Elsevier, Armsterdsam, pp 133–151
140. Moghe AK, Gupta BS (2008) Small-diameter blood vessels by weaving: prototyping and modelling. J Text Inst 99:467–477. https://doi.org/10.1080/00405000701679582
141. Chen Y, Ding X, Li Y et al (2012) A bilayer prototype woven vascular prosthesis with improved radial compliance. J Text Inst 103:106–111. https://doi.org/10.1080/00405000.2011.552956
142. Pourdeyhimi B, Text C (1987) A review of structural and material properties of vascular grafts. J Biomater Appl 2:163–204. https://doi.org/10.1177/088532828700200201
143. Hasegawa M, Azuma T (1979) Mechanical properties of synthetic arterial grafts. J Biomech 12:509–517. https://doi.org/10.1016/0021-9290(79)90039-3
144. Sheridan WS, Duffy GP, Murphy BP (2013) Optimum parameters for freeze-drying decellularized arterial scaffolds. Tissue Eng Part C: Methods 19:981–990. https://doi.org/10.1089/ten.tec.2012.0741
145. Khayat S, Shamloo NA (2019) Bilayered heparinized vascular graft fabricated by combining electrospinning and freeze drying methods. Mater Sci Eng C 94:1067–1076. https://doi.org/10.1016/j.msec.2018.10.016
146. Cao Q, Tao L, Liu M et al (2013) The effect of vacuum freeze-drying and radiation on allogeneic aorta grafts. Mol Med Rep 7:144–148. https://doi.org/10.3892/mmr.2012.1146
147. Carrabba M, Madeddu P (2018) Current strategies for the manufacture of small size tissue engineering vascular grafts. Front Bioeng Biotech 6:41. https://doi.org/10.3389/fbioe.2018.00041
148. Liu S, Hou KD, Yuan M et al (2014) Characteristics of mesenchymal stem cells derived from Wharton's jelly of human umbilical cord and for fabrication of non-scaffold tissue-engineered cartilage. J Biosci Bioeng 117:229–235. https://doi.org/10.1016/j.jbiosc.2013.07.001
149. L'Heureux N, Dusserre N, Konig G et al (2006) Human tissue-engineered blood vessels for adult arterial revascularization. Nat Med 12:361. https://doi.org/10.1038/nm1364
150. Hasan A, Memic A, Annabi N et al (2014) Electrospun scaffolds for tissue engineering of vascular grafts. Acta Biomater 10:11–25. https://doi.org/10.1016/j.actbio.2013.08.022
151. Wang K, Zhang Q, Zhao L et al (2017) Functional modification of electrospun Poly(ε-caprolactone) vascular grafts with the fusion protein VEGF−HGFI enhanced vascular regeneration. ACS Appl Mater Interf 9:11415–11427. https://doi.org/10.1021/acsami.6b16713
152. Fernández-Colino A, Wolf F, Rütten S et al (2019) Small caliber compliant vascular grafts based on elastin-like recombinamers for in situ tissue engineering. Front Bioeng Biotech 7:340. https://doi.org/10.3389/fbioe.2019.00340
153. Jirofti N, Mohebbi-Kalhori D, Samimi A et al (2018) Small-diameter vascular graft using co-electrospun composite PCL/PU nanofibers. Biomed Mater 13:5. https://doi.org/10.1088/1748-605x/aad4b5
154. Ravi S, Chaikof EL (2010) Biomaterials for vascular tissue engineering. Regen Med 5(1):107. https://doi.org/10.2217/rme.09.77
155. Pan Y, Zhou X, Wei Y et al (2017) Small-diameter hybrid vascular grafts composed of polycaprolactone and polydioxanone fibers. Sci Rep 7:3615. https://doi.org/10.1038/s41598-017-03851-1
156. Sirry MS, Zilla P, Franz T (2010) A computational study of structural designs for a small-diameter composite vascular graft promoting tissue regeneration. Cardiovasc Eng Technol 1:269–281. https://doi.org/10.1007/s13239-010-0023-5
157. Yang H, Xu W, Ouyang C et al. (2009) Circumferential compliance of small diameter polyurethane vascular grafts reinforced with elastic tubular fabric. Fibres Text East Eur 17:89–92. http://www.fibtex.lodz.pl/article297.html
158. Do TM, Yang Y, Deng A (2021) Porous bilayer vascular grafts fabricated from electrospinning of the recombinant human collagen (RHC) reptide-based blend. Polymers 13(22):4042. https://doi.org/10.3390/polym13224042
159. Kosolapov AF, Semjonov SL, Denisov AN (2007) Mechanical properties of microstructured high-purity silica fibers. Inorg Mater 43:310–314. https://doi.org/10.1134/S0020168507030181
160. Park S, Kim J, Lee MK et al (2019) Fabrication of strong, bioactive vascular grafts with PCL/collagen and PCL/silica bilayers for small-diameter vascular applications. Mater Des 181:108079. https://doi.org/10.1016/j.matdes.2019.108079
161. Huang R, Gao X, Wang J et al (2018) Triple-layer vascular grafts fabricated by combined E-Jet 3D printing and electrospinning. Ann Biomed Eng 46:1254. https://doi.org/10.1007/s10439-018-2065-z
162. Yadav TC, Srivastava AK, Mishra P et al. (2019) Electrospinning: an efficient biopolymer-based micro- and nanofibers fabrication technique. In Navanietha Krishnaraj Rathinam, Rajesh K. Sani (eds) Next Generation Biomanufacturing Technologies: Washington: ACS Symposium Series, American Chemical Society, pp 209–241. https://doi.org/10.1021/bk-2019-1329.ch010

163. Schröder J, Gruttmann F, Löblein J (2002) A simple orthotropic finite elasto–plasticity model based on generalized stress–strain measures. Comput Mech 30:48–64
164. Sutton MA, Deng X, Liu J et al (1996) Determination of elastic-plastic stresses and strains from measured surface strain data. Exp Mech 36:99–112. https://doi.org/10.1007/BF02328705
165. Akentjew TL, Terraza C, Suazo C et al (2019) Rapid fabrication of reinforced and cell-laden vascular grafts structurally inspired by human coronary arteries. Nat Commun 10:3098. https://doi.org/10.1038/s41467-019-11090-3
166. Centola M, Rainer A, Spadaccio C et al (2010) Combining electrospinning and fused deposition modeling for the fabrication of a hybrid vascular graft. Biofabrication 2:014102. https://doi.org/10.1088/1758-5082/2/1/014102
167. Gupta BS, Kasyanov VA (1997) Biomechanics of human common carotid artery and design of novel hybrid textile compliant vascular grafts. J Biomed Mater Res 34:341–349. https://doi.org/10.1002/(SICI)1097-4636(19970305)34:3%3C341::AID-JBM9%3E3.0.CO;2-K
168. Belleghem SV, Torres L Jr, Santoro M et al (2020) Hybrid 3D printing of synthetic and cell-laden bioinks for shape retaining soft tissue grafts. Adv Funct Mater 30:1907145. https://doi.org/10.1002/adfm.201907145
169. Uden SV, Vanerio N, Catto V et al (2019) A novel hybrid silk-fibroin/polyurethane three-layered vascular graft: towards in situ tissue-engineered vascular accesses for haemodialysis. Biomed Mater 14:025007. https://doi.org/10.1088/1748-605x/aafc96
170. Wu S, Zhou R, Zhou F et al (2020) Electrospun thymosin Beta-4 loaded PLGA/PLA nanofiber/ microfiber hybrid yarns for tendon tissue engineering application. Mater Sci Eng C 10:11068. https://doi.org/10.1016/j.msec.2019.110268
171. Fang Q (2020) Evaluation of a hybrid small caliber vascular graft in a rabbit model. J Thorac Cardiovasc Surg 159:461–473. https://doi.org/10.1016/j.jtcvs.2019.02.083
172. A three-layer fabric woven fabrics and method thereof. Patent No CN105734764B 2017 China. https://patents.google.com/patent/CN105734764A/en
173. Konig G, McAllister TN, Dusserre N et al (2009) Mechanical properties of completely autologous human tissue engineered blood vessels compared to human saphenous vein and mammary artery. Biomaterials 30:1542–1550. https://doi.org/10.1016/j.biomaterials.2008.11.011
174. Bursa J (2002) Modelling of stress-strain states in arteries as a pre-requisite for damage prediction. WIT Trans Eng Sci. https://doi.org/10.2495/DM020481
175. Zhalmuratova D, La TG, Yu KTT et al (2019) Mimicking "J-shaped" and anisotropic stress–strain behavior of human and porcine aorta by fabric-reinforced elastomer composites. ACS Appl Mater Interf 11:33323–33335. https://doi.org/10.1021/acsami.9b10524
176. Leal BBJ, Wakabayashi N, Oyama K et al (2021) Vascular tissue engineering: polymers and methodologies for small caliber vascular grafts. Front Cardiovasc Med 7:592361. https://doi.org/10.3389/fcvm.2020.592361
177. Berger P, Ricco JB, Lung PL et al (2013) Localized argyria caused by metallic silver aortic grafts: a unique adverse effect. Eur J Vasc Endovasc Surg 46(5):565–568. https://doi.org/10.1016/j.ejvs.2013.07.021
178. Pashneh-Tala S, MacNeil S, Claeyssens F (2016) The tissue-engineered vascular graft-past, present, and future. Tissue Eng Part B Rev 22(1):68–100. https://doi.org/10.1089/ten.teb.2015.0100
179. Bhattacharya V, McSweeney PA, Shi Q et al (2000) Enhanced endothelialization and microvessel formation in polyester grafts seeded with $CD34^{+}$bone marrow cells. Blood 95(2):581–585. https://doi.org/10.1182/blood.V95.2.581
180. Toh HW, Toong DWY, Ng JCK et al (2021) Polymer blends and polymer composites for cardiovascular implants. Eur Polym J 146:110249. https://doi.org/10.1016/j.eurpolymj.2020.110249
181. Zhang Y, Wang B, Hu JC et al (2020) 3D composite bioprinting for fabrication of artificial biological tissues. Int J Bioprint 7:299
182. Wu P, Wang L, Li W et al (2020) Construction of vascular graft with circumferentially oriented microchannels for improving artery regeneration. Biomaterials 242:119922. https://doi.org/10.1016/j.biomaterials.2020.119922
183. Wang D, Xu Y, Lin YJ et al (2020) Biologically functionalized expanded polytetrafluoroethylene blood vessel grafts. Biomacromol 21:3807–3816. https://doi.org/10.1021/acs.biomac.0c00897
184. Zhao J, Feng Y (2020) Surface engineering of cardiovascular devices for improved hemocompatibility and rapid endothelialization. Adv Healthc Mater 9:2000920. https://doi.org/10.1002/adhm.202000920
185. Ritchie RO (2011) The conflicts between strength and toughness. Nat Mater 10:817–822. https://doi.org/10.1038/nmat3115
186. Hakoo A (2019) Multi-layer fabrics: the art of weaving several layers in a fabric. https://www.textileschool.com, accessed 20 June 2019
187. Tube-type woven fabric for seamless and its use using the same. Patent No KR20170100955A 2017 South Korea. https://patents.google.com/patent/KR20170100955A
188. A kind of negative Poisson's ratio woven fabric and manufacturing method. Patent No CN106149150B 2019 China. https://patents.google.com/patent/CN106149150B
189. Structure-phase-transition radial-shrinkage-expansion tubular fabric based on soft weft yarn and preparing method thereof. Patent No CN107700023A, 2019, China. https://patents.google.com/patent/CN107700023A
190. Duhaylongsod F (2006) Artificial artificial intelligence: surgeon intuition and computers to predict graft patency. J Thorac Cardiovasc Surg 132:466–467. https://doi.org/10.1016/j.jtcvs.2006.05.016
191. Liu S, Bose R, Ahmed A, Maslow A, Feng Y et al (2020) Artificial intelligence-based assessment of indices of right ventricular function. J Cardiothorac Vasc Anesth 34:2698–2702. https://doi.org/10.1053/j.jvca.2020.01.024
192. Krackov W, Sor M, Razdan R, Zheng H, Kotanko P (2021) Artificial intelligence methods for rapid vascular access aneurysm classification in remote or in-person settings. Blood Purif 50:636–641. https://doi.org/10.1159/000515642
193. Lin CH, Chen WL, Kan CD (2019) Inflow and outflow stenoses screening on biophysical experimental arteriovenous graft using big spectral data and bidirectional associative memory machine learning model. IET Control Theory Appl 4:139–147. https://doi.org/10.1049/iet-cps.2018.5030
194. Chen WL, Kan CD, Lin CH (2017) Assessment of inflow and outflow stenoses using big spectral data and radial-based colour relation analysis on in vitro arteriovenous graft biophysical experimental model. IET Control Theory Appl 2:10–19. https://doi.org/10.1049/iet-cps.2016.0040
195. Lin CH, Wu JX, Kan CD, Chen PY, Chen WL (2021) Arteriovenous shunt stenosis assessment based on empirical mode decomposition and 1D-convolutional neural network: clinical trial stage. Biomed Signal Process Control 66:102461. https://doi.org/10.1016/j.bspc.2021.102461
196. Wu X, Zhou H (2016) Control and simulation of head temperature field of vascular 3D print based on beckhoff. Proceedings of the 28th Chinese control and decision conference p.626–631. https://doi.org/10.1109/CCDC.2016.7531061